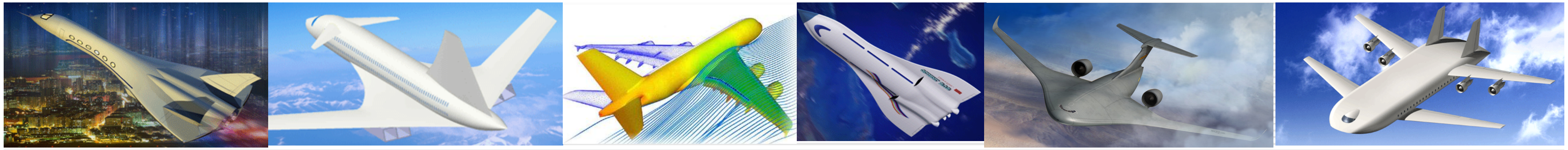

Games strategies and Evolutionary Algorithms for CFD optimization.

Applications: Drag reduction of a Natural Laminar Airfoil using an Active Bump at Transonic Flow Regimes (1) , Distributed propulsion (2) and Structural Engineering (3)

Jacques Periaux°, 唐智礼(Z.L. Tang)*, 陈永彬(Y.B. Chen)*

° International Center for Numerical Methods in Engineering (CIMNE/UPC)

* Nanjing University of Aeronautics & Astronautics (NUAA) applications (1) and (2)

Credit for application (3):

David Greiner , Jose M. Emperador, Blas Galvan, Gabriel Winter , ULPGC

UNIVERSIDAD DE LAS PALMAS DE GRAN CANARIA

CIMNE

XVIII Spanish-French School Jacques Louis Lions about Numerical Simulation in Physics and Engineering

Las Palmas de Gran Canaria, Spain, June 25-29, 2018

Content

This lecture presents :

1) Theoretical ingredients coupling EAs with games
2) Applications of Advanced Evolutionary Methods to Aeronautics/Structure Design with hybridized Game/GAs

1) Motivation: MASTERING COMPLEXITY, A COLLABORATIVE WORK....

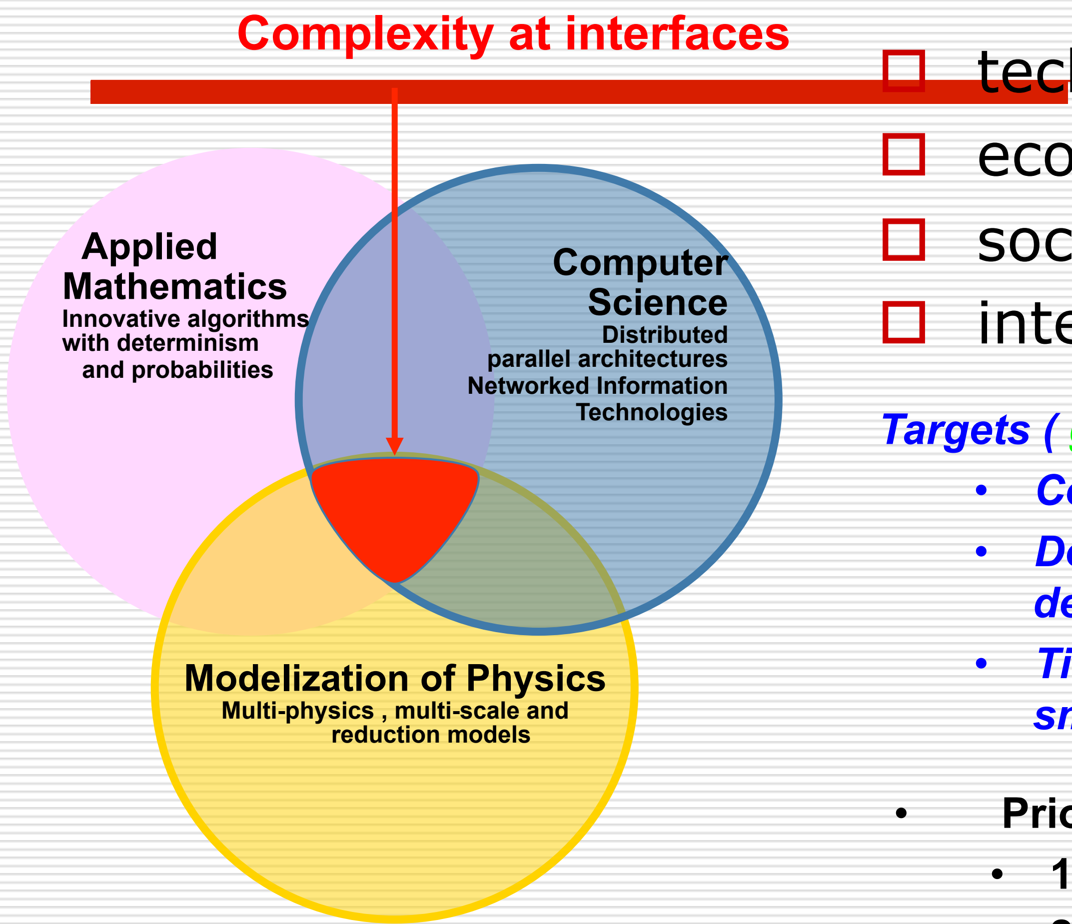

- technological constraints
- economical constraints
- societal constraints (H2020)
- integrated systems

Targets (greener, safer digitalized products)

- *Computational multi disciplinary tools*
- *Decision maker algorithms for the design of industrial products*
- *Time and cost reduction with digitalized smart and intelligent systems*

- **Priorities**
  - **1) Robustness (global solutions)**
  - **2) Affordable cost and efficiency**
  - **3) Transport obility**

THE CONTEXT….

Multi Disciplinary

Search Space – Large
Multimodal
Non-Convex
Discontinuous

Share data knowledge: different cultures and technologies connected

Integration of software with interfaces and human factors

Trade off between conflicting Requirements

EVOLUTIONARY ALGORITHMS (60’) (John Holland:adaptation David Goldberg : optimisation

Traditional Gradient Based methods for MDO cannot capture optimal solution 100% of the cases

if the search space is in particular:

- **Large and hilly**
- **Multimodal**
- **Non-Convex**
- **Many Local Optima**
- **Discontinuous**

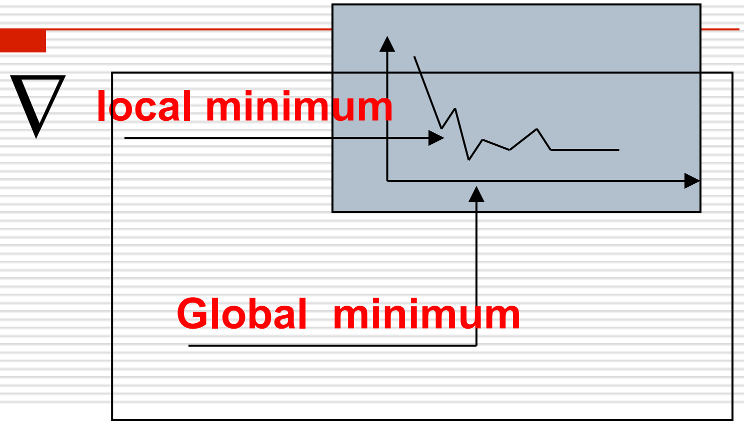

A real aircraft design optimization might exhibit one or several of these characteristics

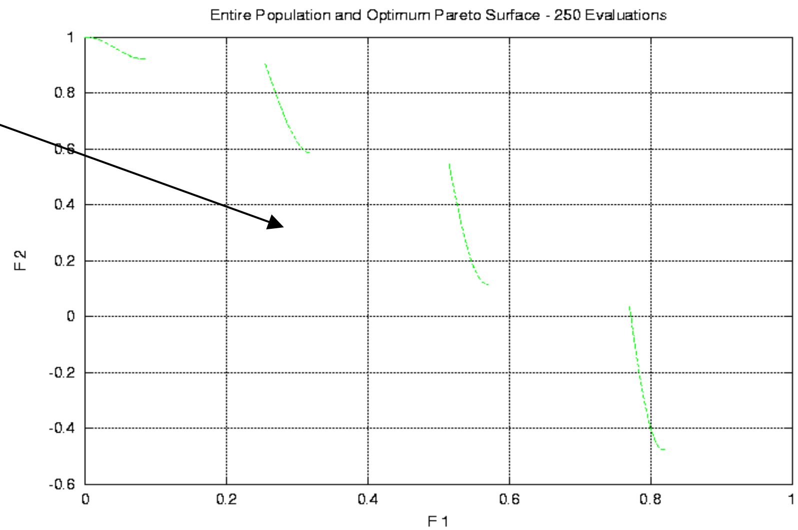

CIMNE

MECHANICS OF GAS: pioneered by J. Holland in the 60' with the binary coding of variables

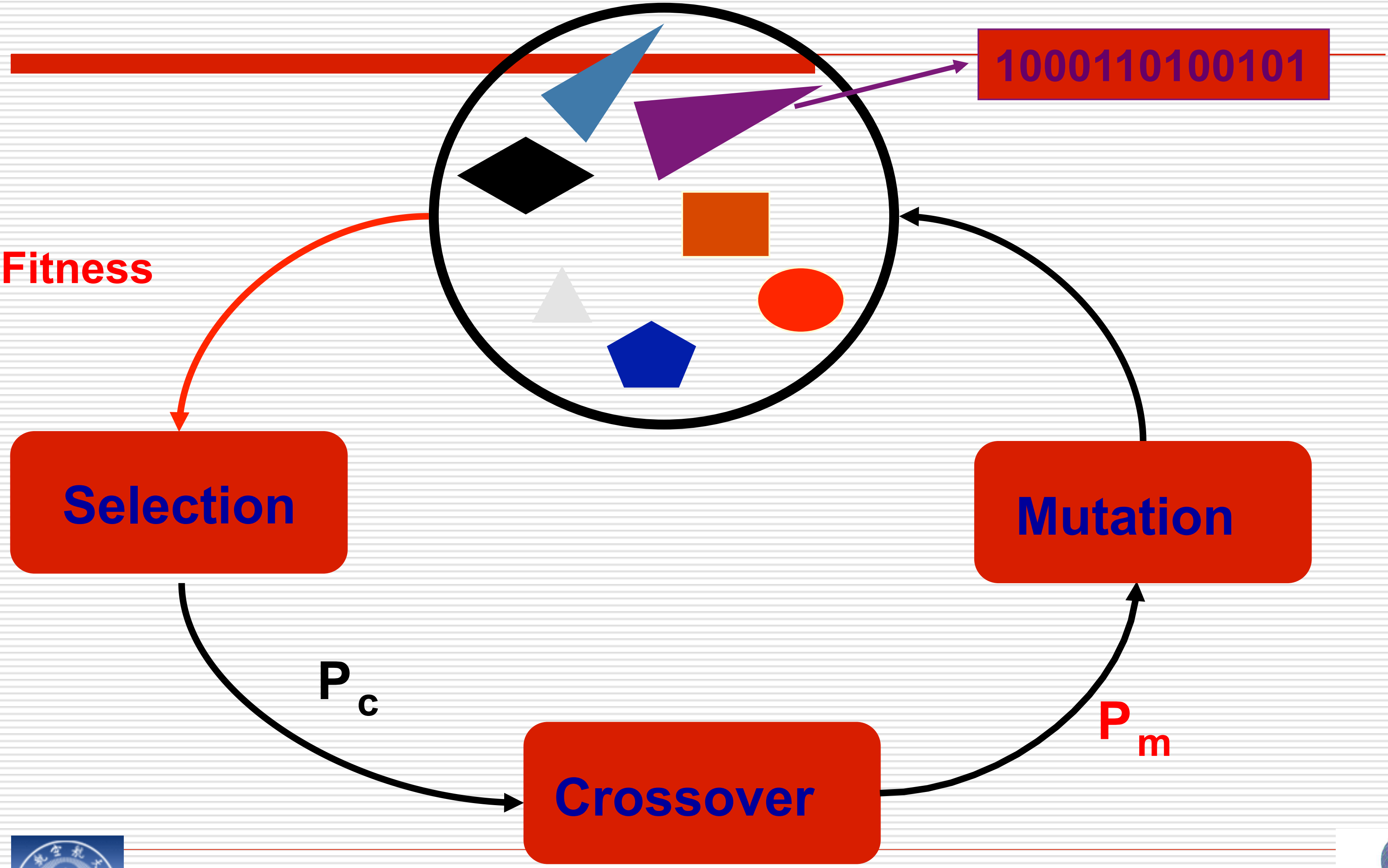

Genetic Algorithms (GAs): parameters

Population size: 30-100 , problem dependent

Cross over rate: Pc= 0.80-0.95

Mutation rate: Pm= 0.001- 0.01

GENETIC ALGORITHMS :
Example of a chromosome or individual

In this example: A chromosome or an individual are *the control points (yi)* that define the airfoil shape

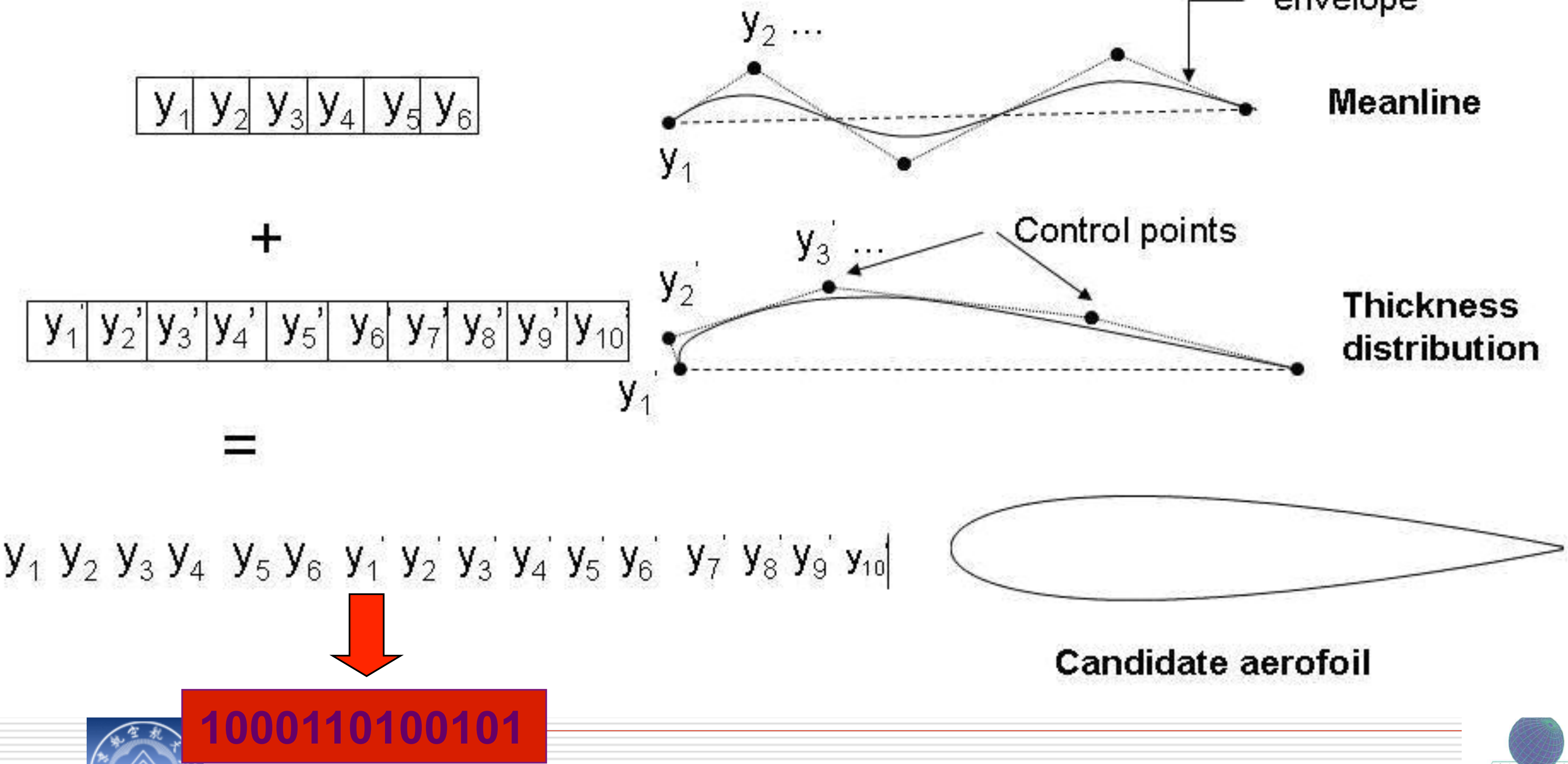

MULTI-OBJECTIVE OPTIMISATION (1)

- Aeronautical design problems require more and more multi objective optimization with constraints.

- This situation occurs when two or more objectives that cannot be combined rationally. Some examples :

  - **Drag at two different values of lift.**
  - **Efficiency and noise**
  - **Drag and thickness.**
  - **Drag and RCS signature**

  ....

MULTI-OBJECTIVE OPTIMISATION

Different Multi-Objective approaches

- Aggregated Objectives, main drawback is loss of information and the a-priori biased choice of weights.

- Game Theory (von Neumann)
  - Game Strategies
    - Cooperative Games - Pareto
    - Competitive Games - Nash
    - Hierarchical Games - Stackelberg

- Vector Evaluated GA (VEGA) Schaffer,85

MULTI-OBJECTIVE OPTIMISATION

Impossible d'afficher l'image. Votre ordinateur manque peut-être de mémoire pour ouvrir l'image ou l'image est endommagée. Redémarrez l'ordinateur, puis ouvrez à nouveau le fichier. Si le x rouge est toujours affiché, vous devrez peut-être supprimer l'image avant de la réinsérer.

Maximise/ Minimise $f_i(x) \quad i = 1 \ldots N$

Subjected to constraints

$$g_i(x) = 0 \quad j = 1 \ldots N$$

$$h_k(x) \leq 0 \quad k = 1 \ldots K$$

- $f_i(x)$ → Objective functions, output (e.g. cruise efficiency).
- *x:* vector of design variables, inputs (e.g. aircraft/wing geometry)
- *g(x)* equality constraints and *h(x)* inequality constraints: (e.g. element von Mises stresses); in general they are nonlinear functions of the design variables.

GAME STRATEGIES

- Theoretical foundations: **Von Neumann**
- Applications to Economics and Politics: **Von Neuman, Pareto, Nash, Von Stackelberg**
- Decentralized optimization methods:

***Lions*-Bensoussan-Temam** in Rairo (1978, **G. Marchuk**, *J.L. Lions*, eds)

In this lecture: introduction and use of Games strategies in Engineering for solving Multi Objective Optimization Problems

GAME STRATEGIES: NOTATIONS

- For a game with 2 players, A and B
- For A
  - Objective function $f_A(x,y)$
  - A optimizes vector x
- For B
  - Objective function $f_B(x,y)$
  - B optimizes vector y

$$\overline{A} = \text{set of possible strategies for A}$$

$$\overline{B} = \text{set of possible strategies for B}$$

Pareto Dominance

- Pareto Optimality (minimization, 2 Players A and B).

(x^*,y^*) o optimal if and only if:

$$\forall (x,y) \in \overline{A} \times \overline{B}, \begin{cases} f_A(x^*,y^*) \le f_A(x,y) \\ f_B(x^*,y^*) \le f_B(x,y) \end{cases}$$

- **Pareto Dominance (for n players ($P_1,\ldots,P_n$)**
  - **Player P_i has objective f_i and controls v_i**
  - **(v_1*,..,v_k*,..,v_n*) dominates (v_1,..,v_k,..,v_n) iff:**

$$\begin{cases} \forall i, f_i(x_1^*,\ldots,x_k^*,\ldots,x_n^*) \le f_i(x_1,\ldots,x_k,\ldots,x_n) \\ \exists i, f_i(x_1^*,\ldots,x_k^*,\ldots,x_n^*) < f_i(x_1,\ldots,x_k,\ldots,x_n) \end{cases}$$

MULTIPLE OBJECTIVE OPTIMIZATION

- Linear Combination of criteria (aggregation)

$$C = \sum_{i=1}^{n} \omega_i \cdot c_i$$

BUT:

- **Dimensionless number**
- **Heavy bias by the choice of the weights**

BETTER:

- **VEGA (Vector-Evaluated GA)** [Schaffer, 85]
  - **bias on the extrema of each objective**

Pareto Front

- **Pareto Optimality:**
  - a strategy $(v_1^*,..,v_k^*,..,v_n^*)$ is Pareto-optimal if it is not dominated

- **Pareto Front:**
  - The set of all NON-DOMINATED strategies

Nash Equilibrium

- Competitive symmetric games [Nash, 1951]

- For 2 Players A and B:

$$f_A(\vec{x}^*, \vec{y}^*) = \inf_{x \in \bar{A}} f_A(x, \vec{y}^*)$$

$$f_B(\vec{x}^*, \vec{y}^*) = \inf_{y \in \bar{B}} f_B(\vec{x}^*, y)$$

- For n Players :

$$\forall i, \forall v_i, f_i(\vec{v}_1^*, \ldots, \vec{v}_{i-1}^*, \vec{v}_i^*, \vec{v}_{i+1}^*, \ldots, \vec{v}_n^*) \\ \leq f_i(\vec{v}_1^*, \ldots, \vec{v}_{i-1}^*, \vec{v}_i, \vec{v}_{i+1}^*, \ldots, \vec{v}_n^*)$$

« When no player can further improve his criterion, the system has reached a state of equilibrium named Nash equilibrium ”

How to find a Nash Equilibrium ?

- Let D_A be the rational reaction set for A, and D_B the rational reaction set for B.

$$\begin{cases} D_A = \left\{ (x^*, y) \in \bar{A} \times \bar{B} \right\} \text{ such that } f_A(x^*, y) \le f_A(x, y) \\ D_B = \left\{ (x, y^*) \in \bar{A} \times \bar{B} \right\} \text{ such that } f_B(x, y^*) \le f_B(x, y) \end{cases}$$

- **Which can be formulated**:

$$\begin{cases} D_A = \left\{ x, \dfrac{\partial f_A(x, y)}{\partial x} = 0 \right\} \\ D_B = \left\{ y, \dfrac{\partial f_B(x, y)}{\partial y} = 0 \right\} \end{cases}$$

- **A strategy pair (x*,y*)**
- **is a Nash Equilibrium**

$$(x^*, y^*) \in D_A \cap D_B$$

[Sefrioui & Periaux, 97]

X Y

Player 1 Player 2

Nash GAs

Player 1 = Population 1

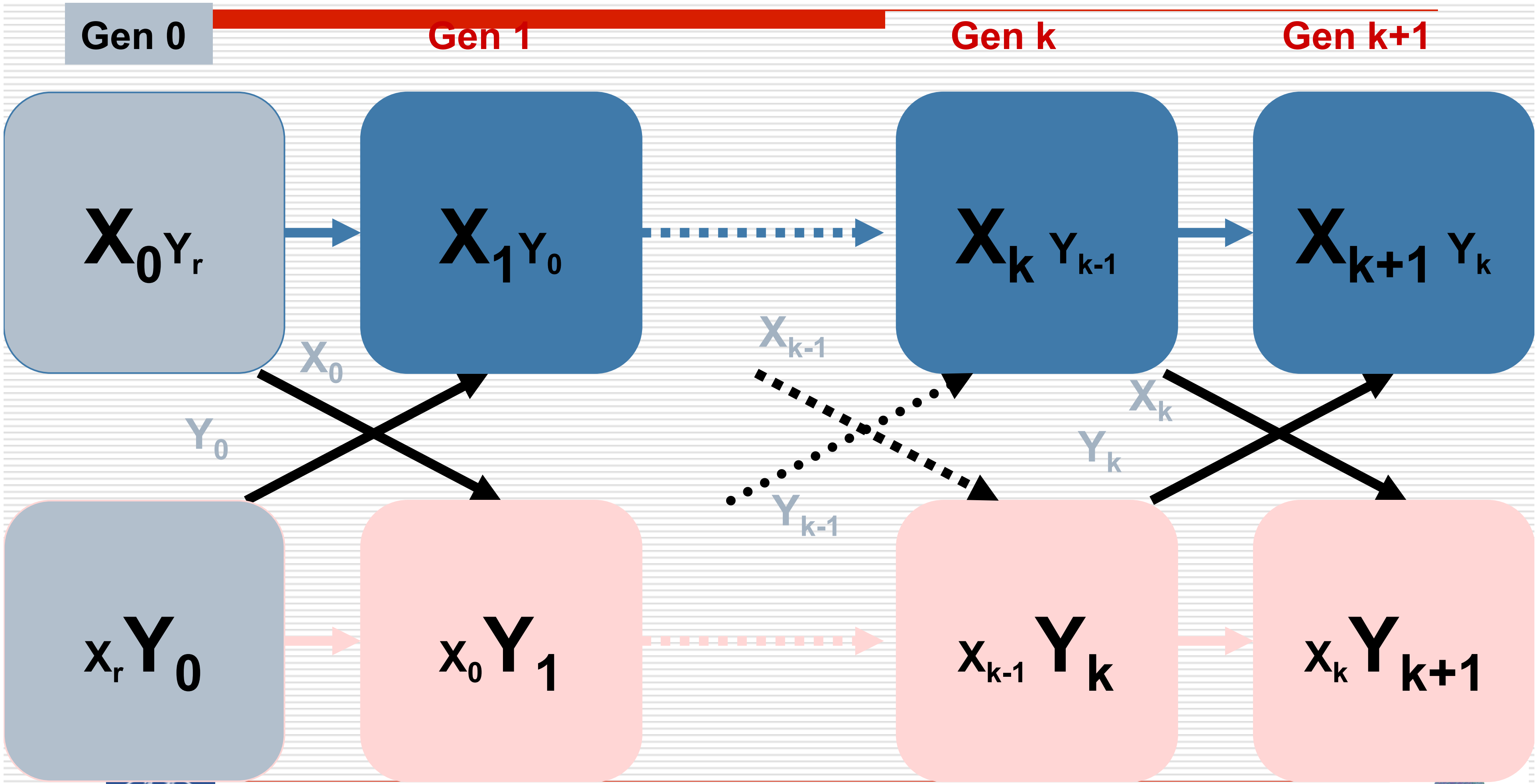

Player 2 = Population 2

Stackelberg Games

Hierarchical strategies

- **Stackelberg game with A leader and B follower :**

minimize $f_A(x,y)$ with y in D_B

- **Stackelberg game with B leader and A follower :**

$$\min_{x \in D_A,\, y \in \bar{B}} f_B(x,y)$$

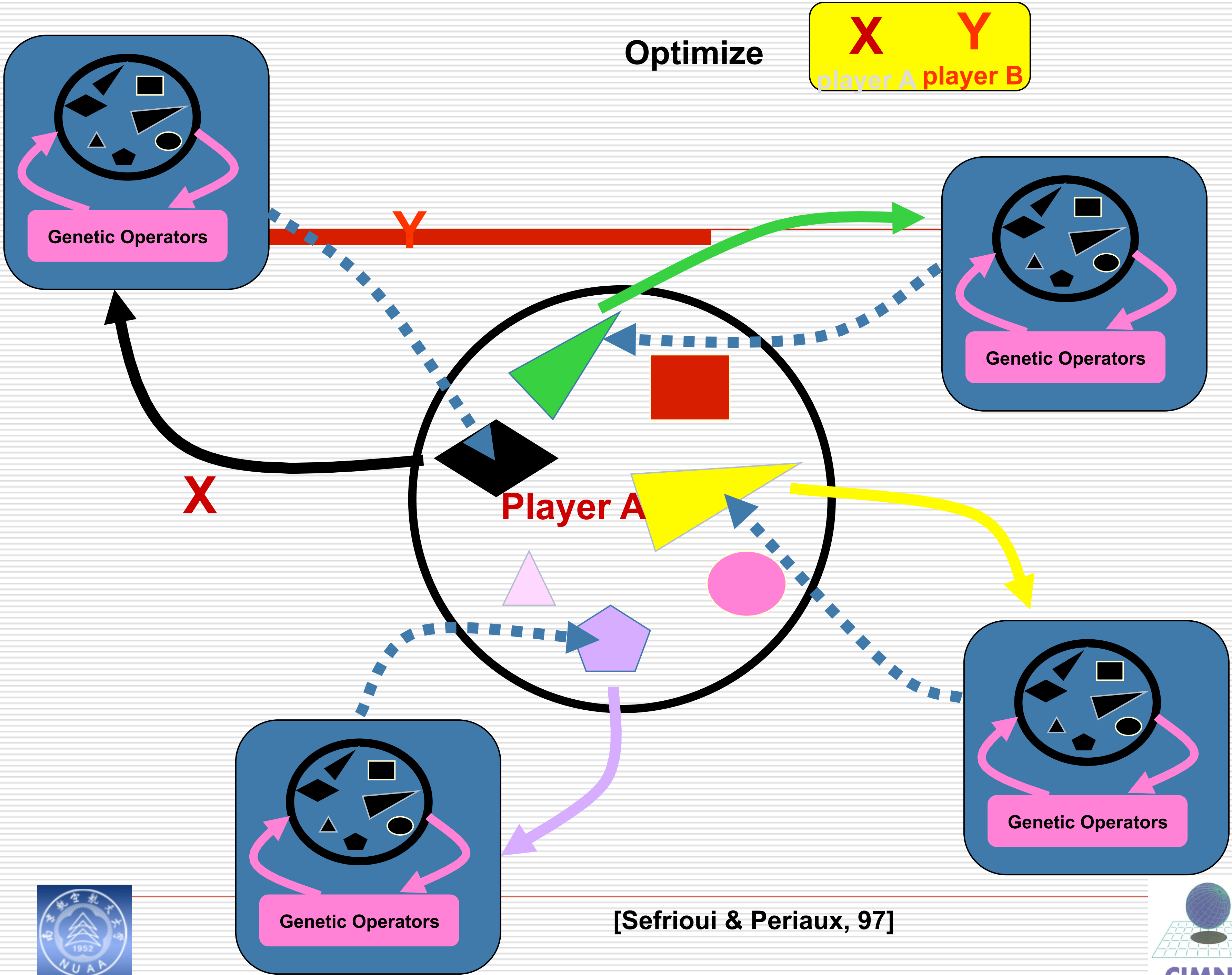

[Sefrioui & Periaux, 97]

Example: Two objective optimization using Pareto, Nash and Stackelberg games on a simple test case

- Let us consider a game with 2 players A and B, with the following objective functions

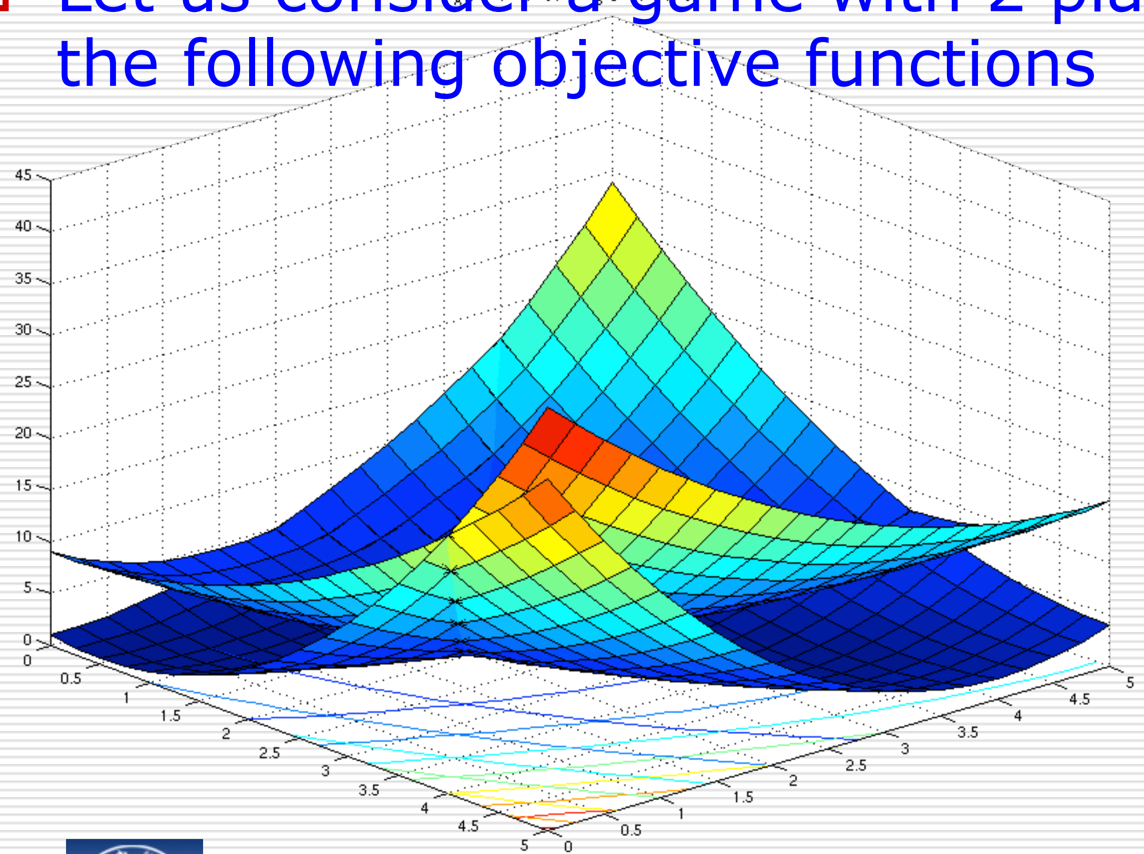

$$f_A = (x-1)^2 + (x-y)^2$$
$$f_B = (y-3)^2 + (x-y)^2$$

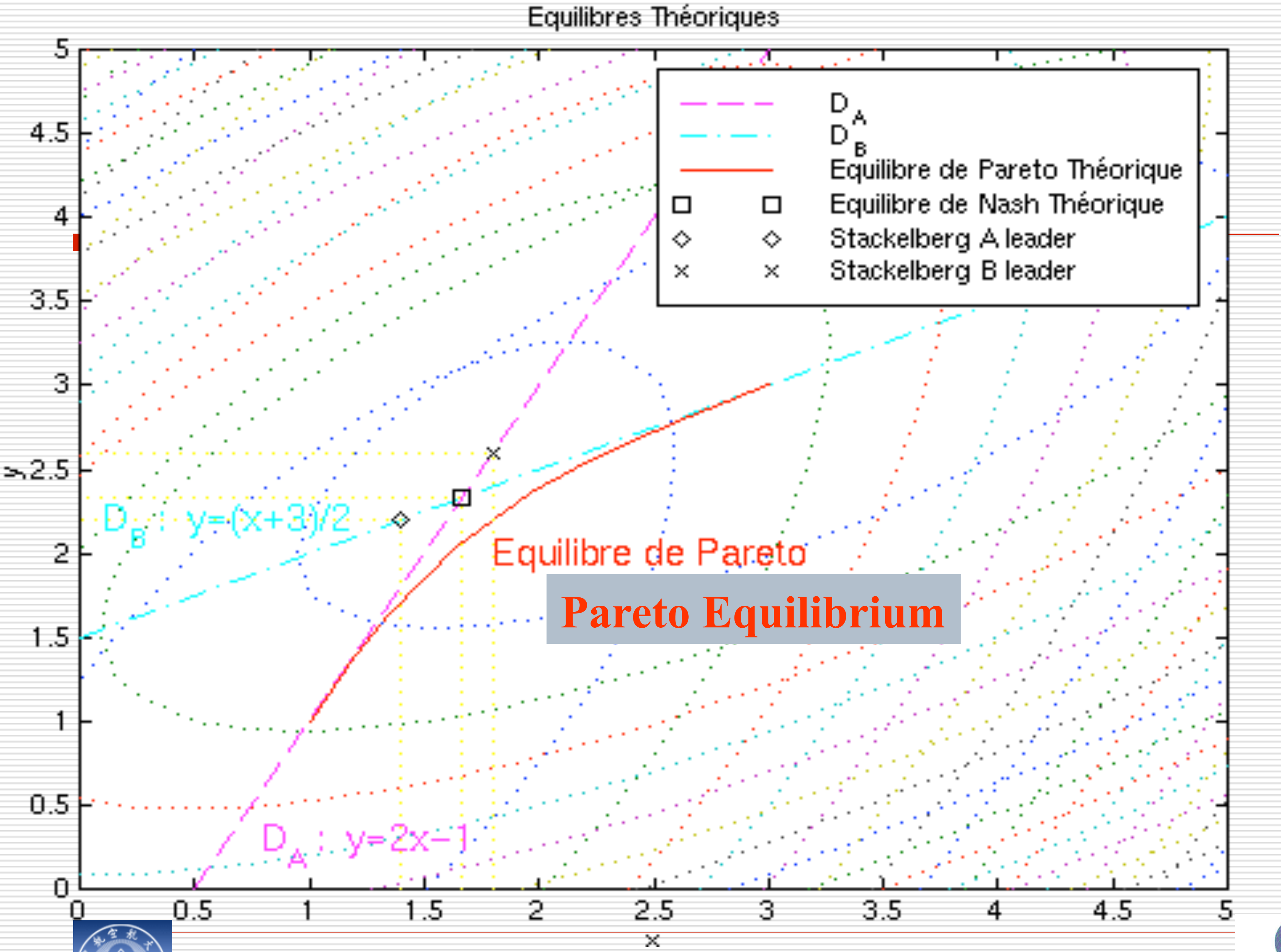

Pareto Equilibrium

Optimization with GAs

- optimize the function f_A and f_B with the GAs optimization tools presented earlier
  - using a (Pareto game/GAs)
  - using a (Nash game/GAs)
  - using a (Stackelberg game/GAs)

Nash GA : convergence

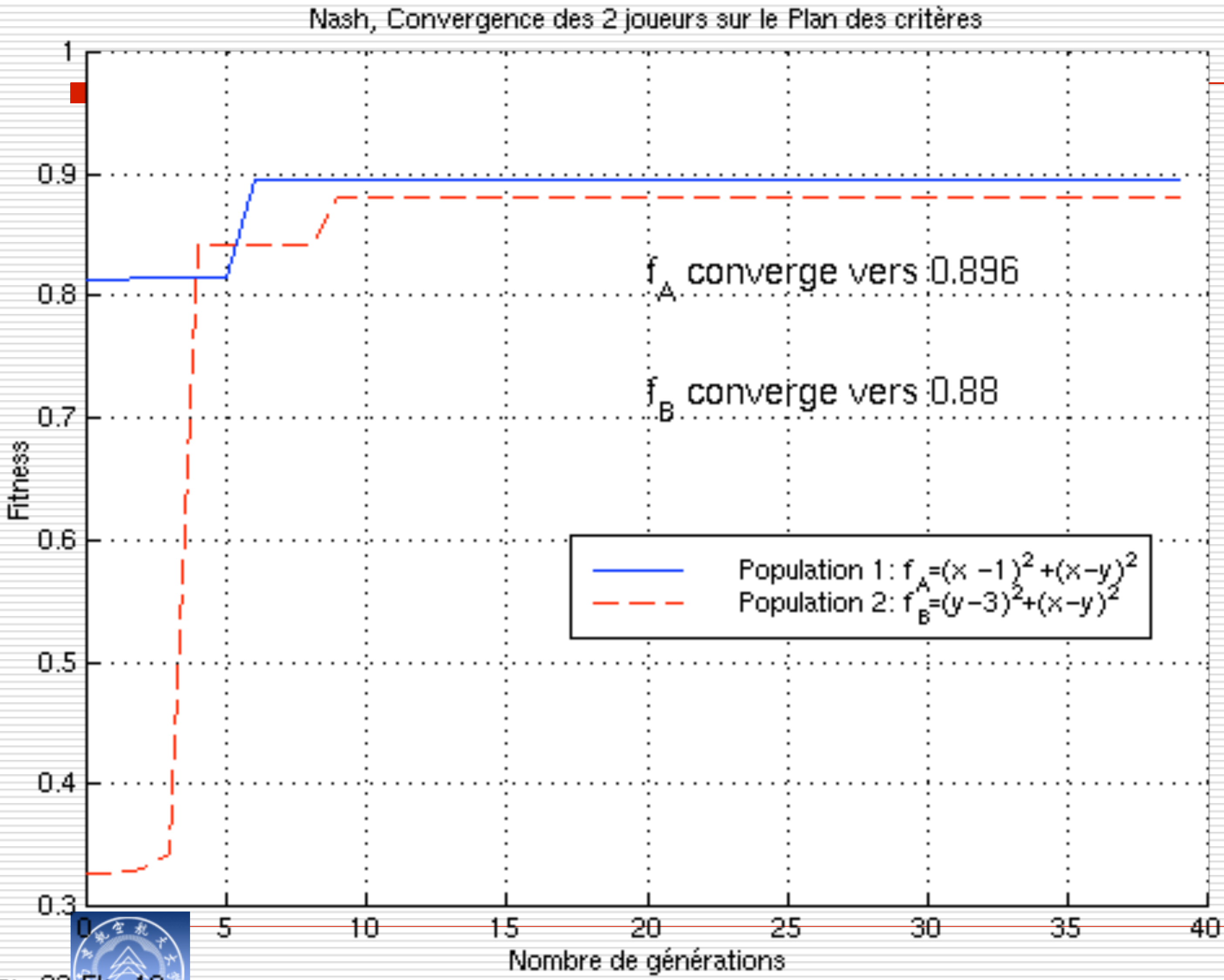

Nash GA: Convergence (2)

- f_A converges towards 0.896 and f_B towards 0.88
- Both those are the values on the objective plane!
- we can check that

$$f_A\left(\frac{5}{3},\frac{7}{3}\right)=0.896 \quad \text{and} \quad f_B\left(\frac{5}{3},\frac{7}{3}\right)=0.88$$

- **Conclusion: the Nash GA finds the analytic Nash Equilibrium**
- **Specifications:**
  - **2 populations, each of size 30**
  - **P_c=0.95 P_m=0.01**
  - **Exchange frequency : every generation !**
  - **(x,y) in [-5,5]x[-5,5]**

Nash GA : convergence

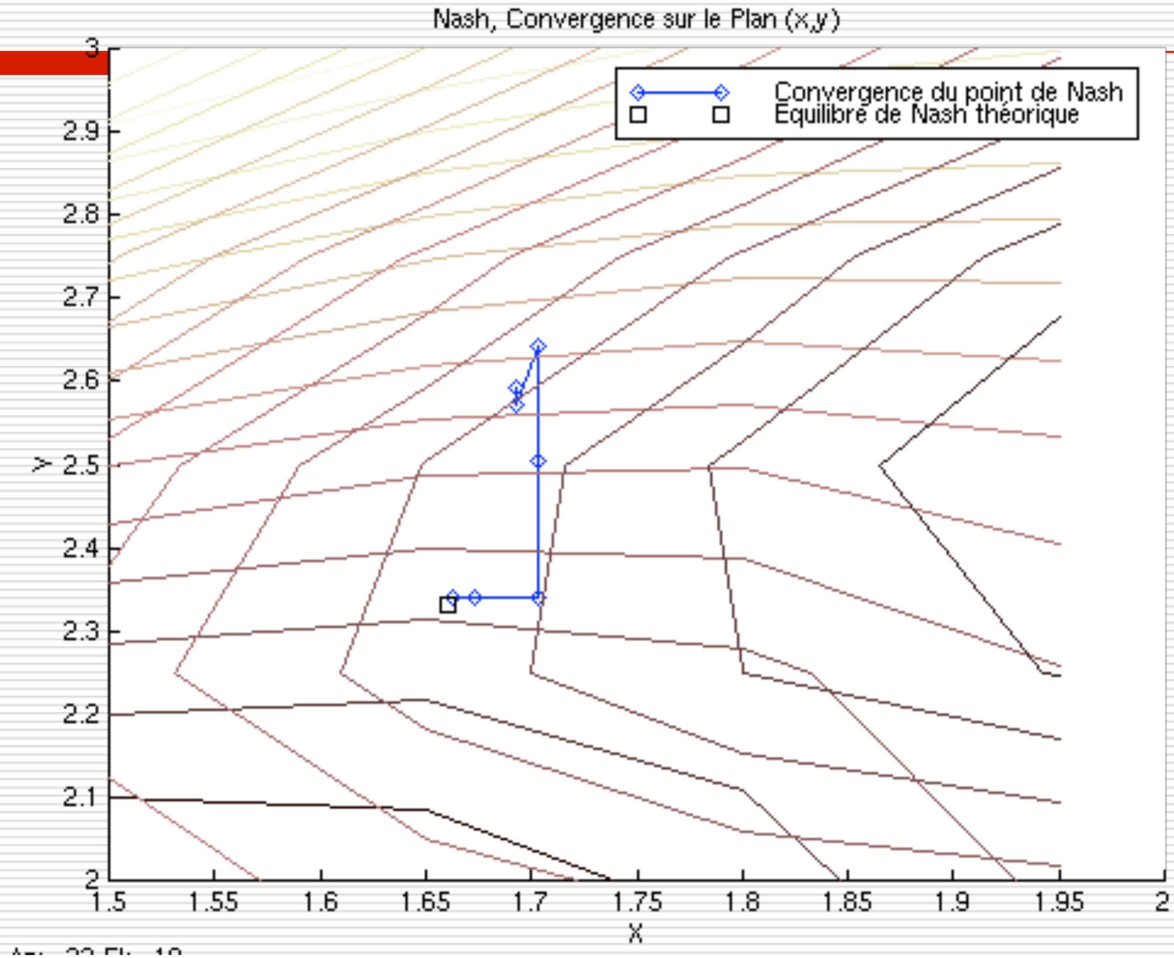

GAs Pareto Front

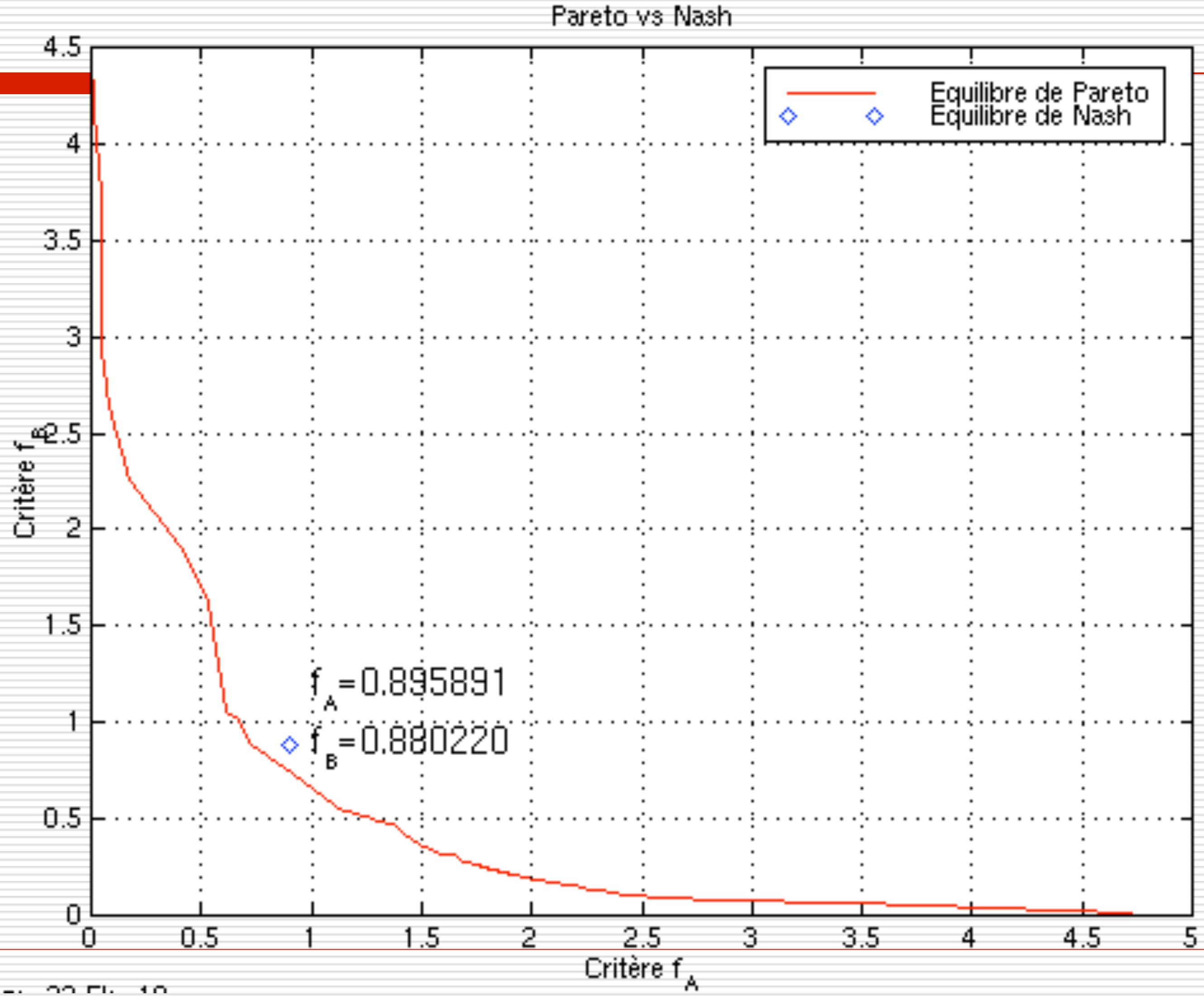

Stackelberg GA : convergence

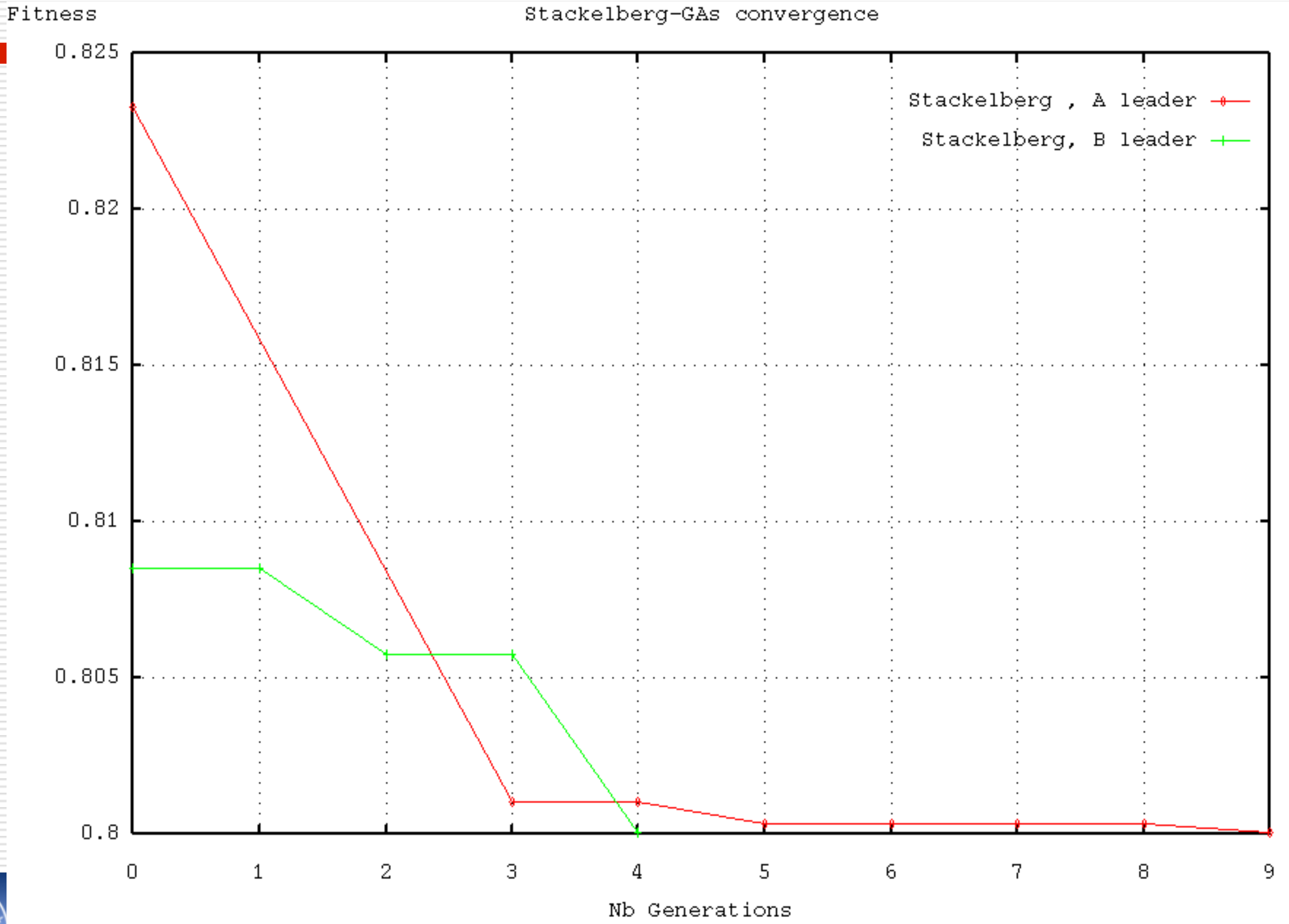

Stackelberg GA : convergence (3)

- In both cases (with either A or B leaders), the algorithms converges towards 0.8 but in the objective plane.
- In the (x,y) plane, we can see that the first game converges towards (1.4,2.2) and that the second game converges towards (1.8,2.6)

Converged games solutions for GAs vs analytical approaches

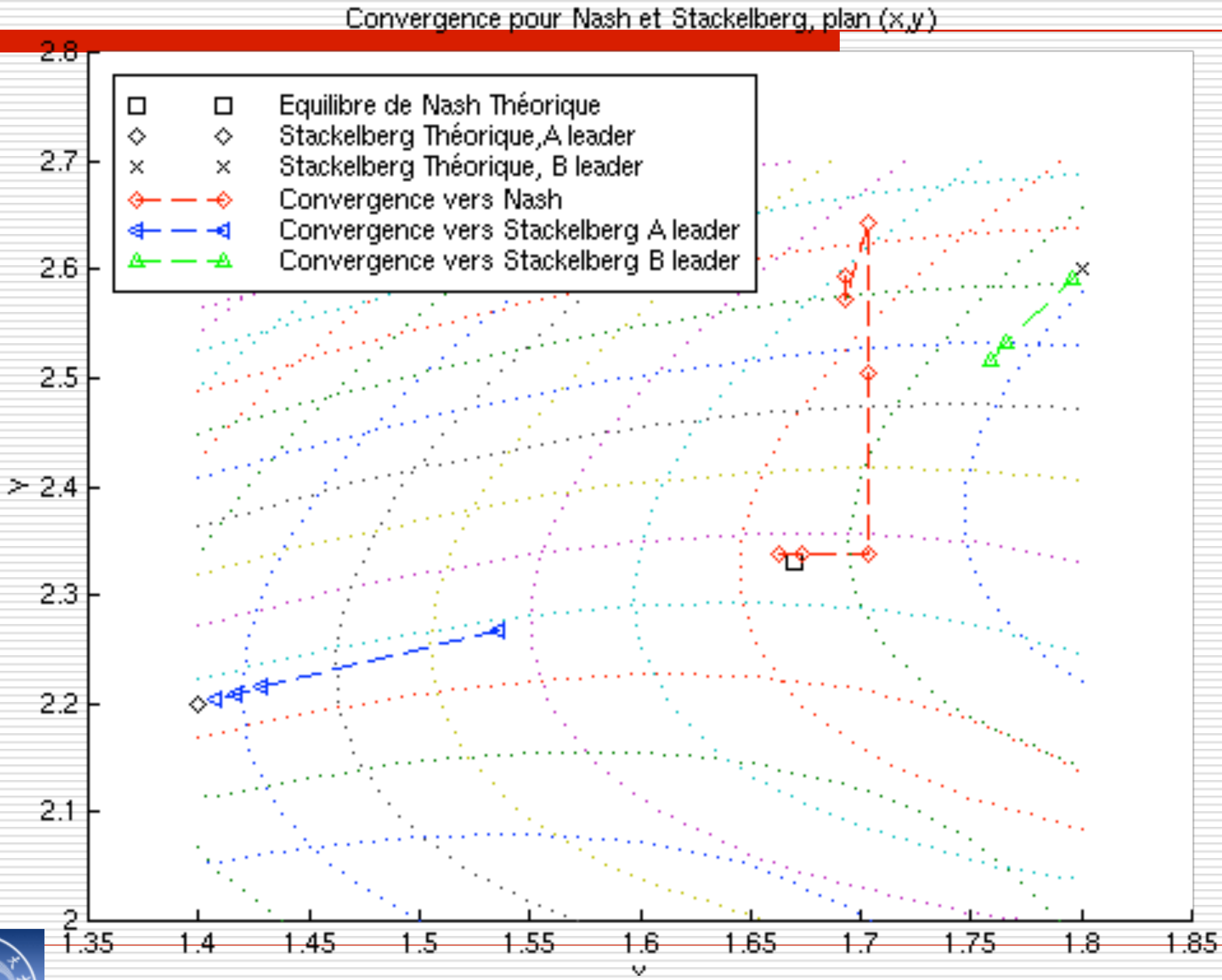

Equilibria of the three games

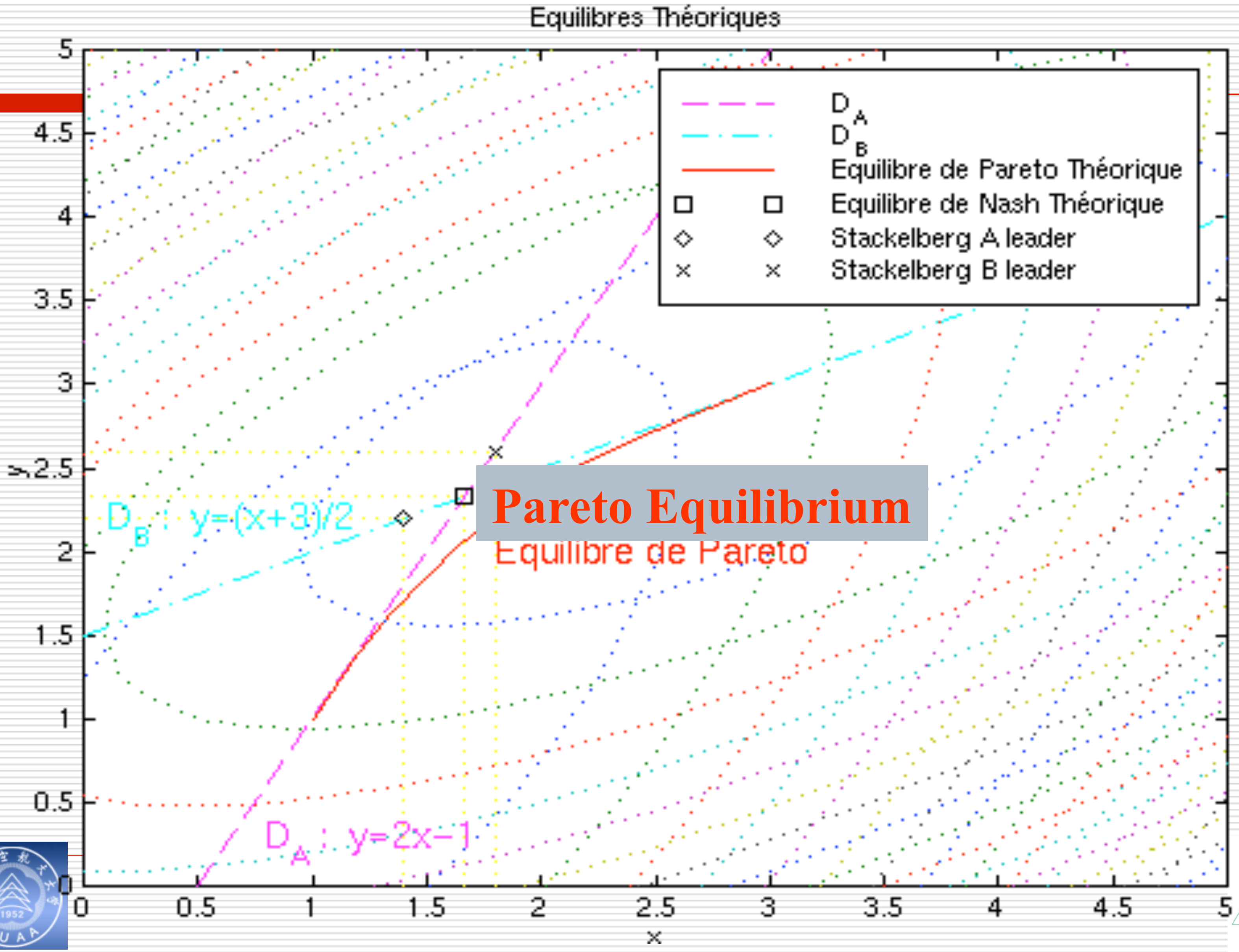

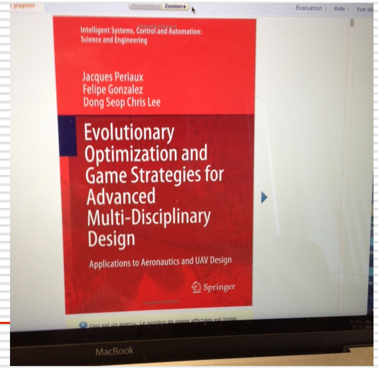

Some REFERENCES:

1. Hansen, N. and Ostermeier, A. *Completely Derandomised Self-Adaption in Evolution Strategies*, in Evolutionary Computation, volume 9(2), pages 159–195. MIT Press, 2001.

2. Gonzalez, L. F. *Robust Evolutionary Method For Multi-objective And Multidisciplinary Design Optimisation In Aeronautics*, The University of Sydney, 2005.

3. Gonzalez, L.F , Whitney, E.J. , Periaux, J., Sefrioui, M. and Srinivas, K. *A Robust Evolutionary Technique for Inverse Aerodynamic Design, Design and Control of Aerospace Systems Using Tools from Nature*. Proceedings of the 4th European Congress on Computational Methods in Applied Sciences and Engineering, Volume II, ECCOMAS 2004, Jyvaskyla, Finland, July 24-28, 2004 m Eds:P. Neittaanmaki mT. Rossim S. Korotovm E. Onate m J. Periaux and D. Knorzer, University of Jyvaskyla, Jyvaskyla, 200$m CD ISBN 951-39-1869-6.

4. González, L., Whitney, E., Srinivas, K. and Periaux, J. *Multidisciplinary Aircraft Design and Optimisation Using a Robust Evolutionary Technique with Variable Fidelity Models*, AIAA Paper 2004-4625, In CD Proceedings 10th AIAA/ISSMO Multidisciplinary Analysis and Optimization Conference, Aug. 30 - Sep. 1, 2004, Albany, NY.

5. Whitney, E. J. *A Modern Evolutionary Technique for Design and Optimisation in Aeronautics,* PhD Thesis, The University of Sydney, 2003.

6. Whitney, E., Sefrioui, M., Srinivas, K. and Périaux, J., *Advances in Hierarchical, Parallel Evolutionary Algorithms for Aerodynamic Shape Optimisation*, JSME (Japan Society of Mechanical Engineers) International Journal, Vol. 45, No. 1, 2002

7. D.S. Lee, *Uncertainty Based MultiObjective and Multidisciplinary Design Optimization in Aerospace Engineering*, PhD, University of Sydney, NSW, Australia , 2008

8. J.Periaux, F. Gonzalez, DS. C.Lee, *Advanced Evolutionary Algorithms and Games Strategies for Multidisciplinary Design : Application to Aeronautics*, Springer , 2015

CIMNE

2. *Applications* of Advanced Evolutionary Optimization Methods to Aeronautics Design with EAs

- ***(2) Drag reduction of a Natural Laminar Airfoil using an Active Bump at Transonic flow regimes***

(J.Periaux, Z.Tang, Y.B. Chen, Lianhe Zhang)

Outline

1. Motivation

2. Flow field simulation and laminar-turbulent transition prediction on an airfoil

3. Definition of the Natural Laminar Flow (NLF) airfoil shape design optimization

4. General game mathematical formulations for multi-objective optimization

5. Numerical implementation of the two objective evolutionary shape optimization of NLF airfoil and SCB using game strategies (Pareto, Nash ,Stackelberg)

6. Results of optimization and analysis for different games

7.Conclusion and perspectives

1. Motivation

Drag breakdown typical of a large modern swept-wing aircraft

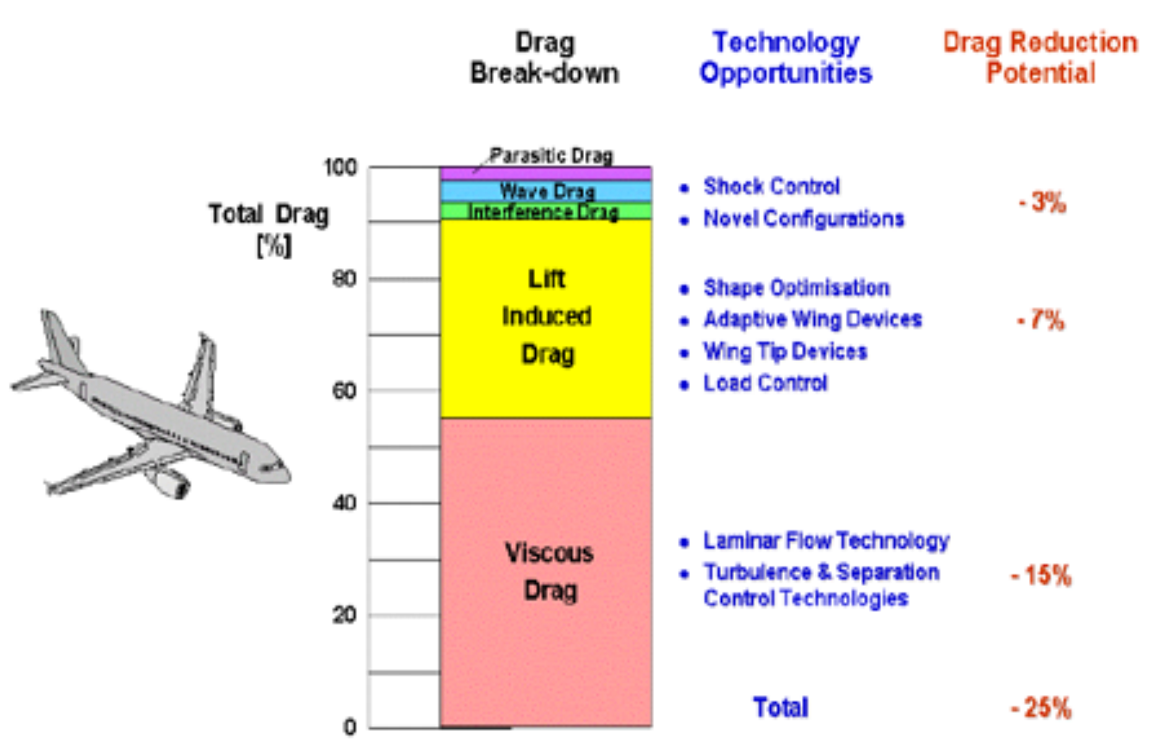

- *In order to improve the performances of a civil aircraft at transonic regimes, it is critical to develop new computational optimization methods to reduce friction drag.*
- *At high Reynolds numbers, LFC technologies and NLF airfoil/wing design remain effcient methods to reduce the turbulence skin friction*

Typical Drag Reduction Methods

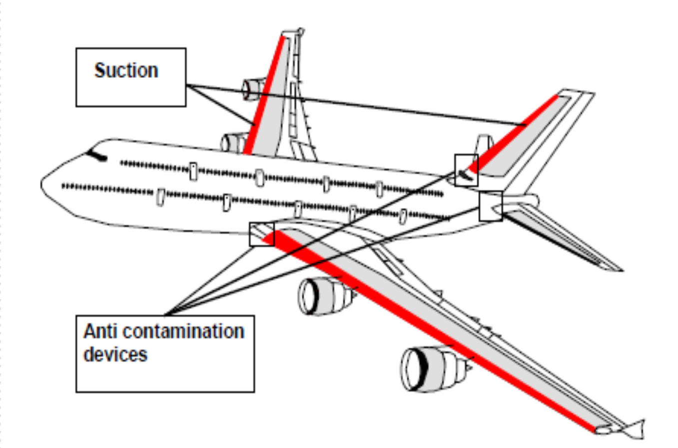

Laminarity

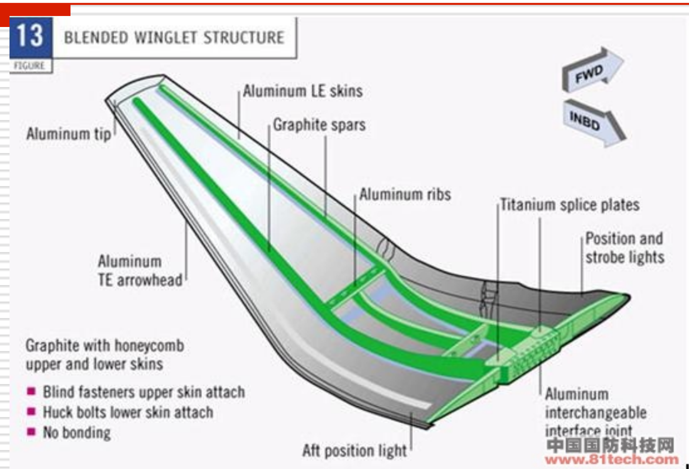

Blended Winglet

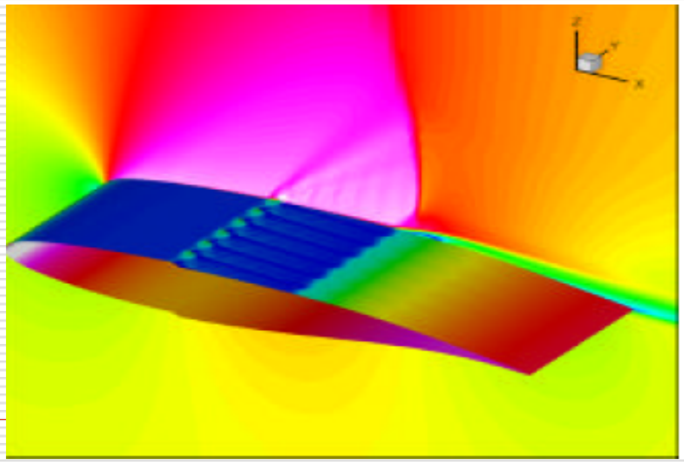

Vortex Generator

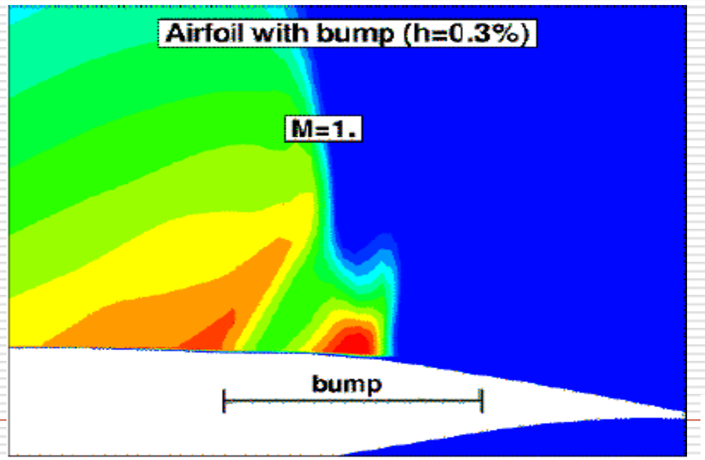

Bump for Shock Wave Control

How to delay transition on an airfoil ? ? ?

- LFC (Laminar Flow Control): **modifying the shape of the boundary layer velocity profile !**
  by applying small amount of suction or blowing at the wall (active device)

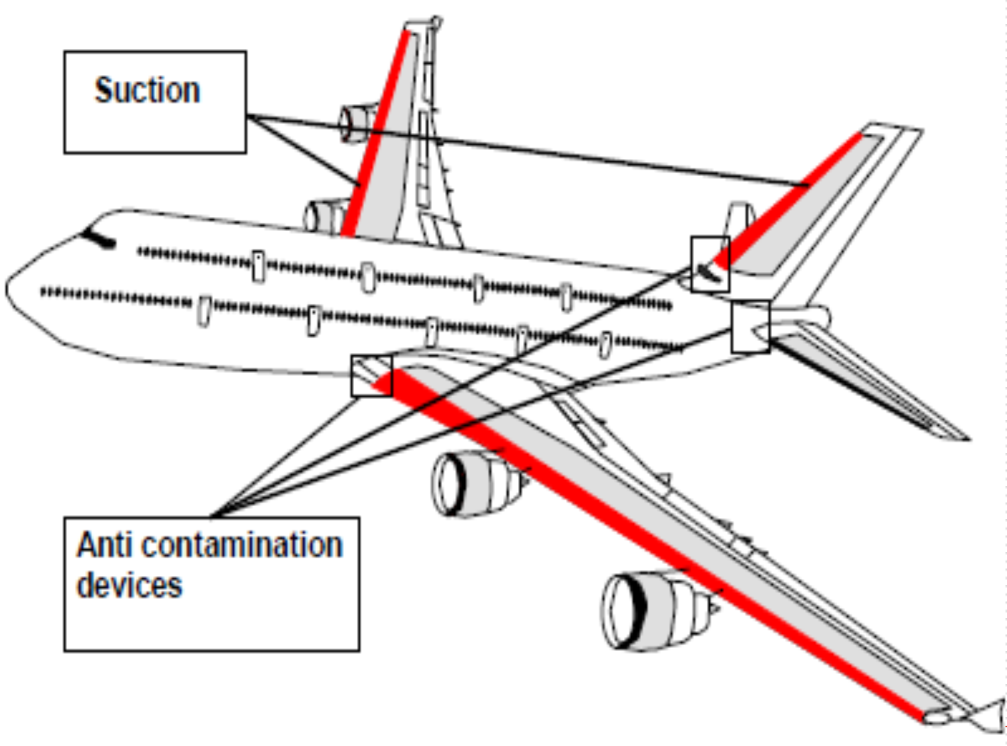

- **NLF (Natural Laminar Flow): optimizing the airfoil/wing shape to get a favorable pressure distribution and improve the boundary layer stability : it is the presented approach !**

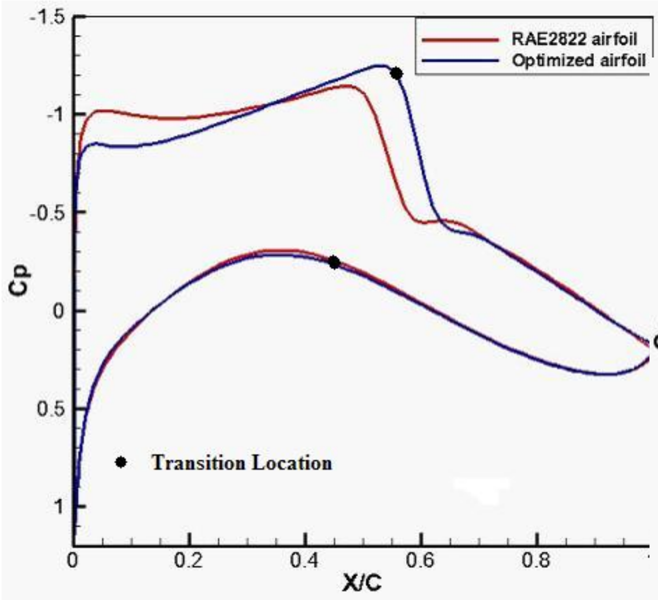

1

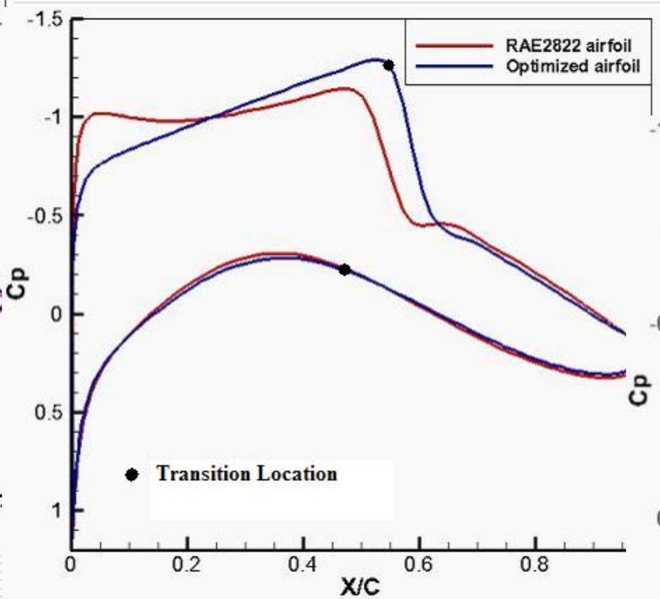

2

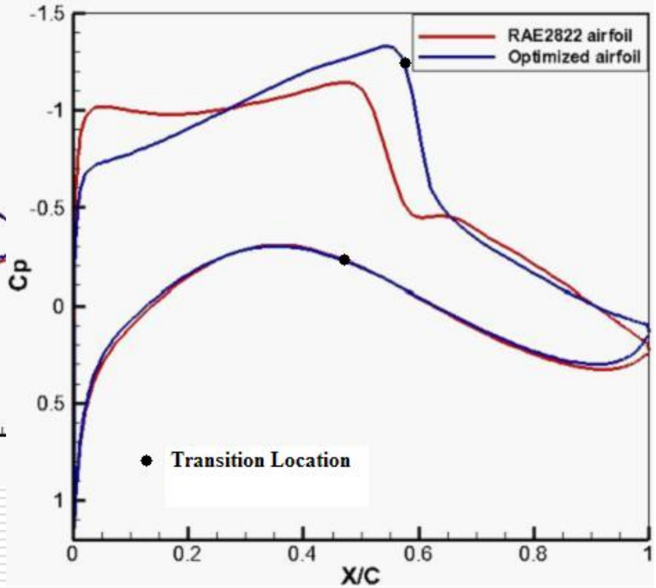

But the larger the region of laminar flow is, the stronger the shock wave is ! (compare figures 1-2-3)

3

How to overcome the conflict between laminar flow and shock wave ? ? ?

➔ *Install a bump at the location of the shock wave !!!*

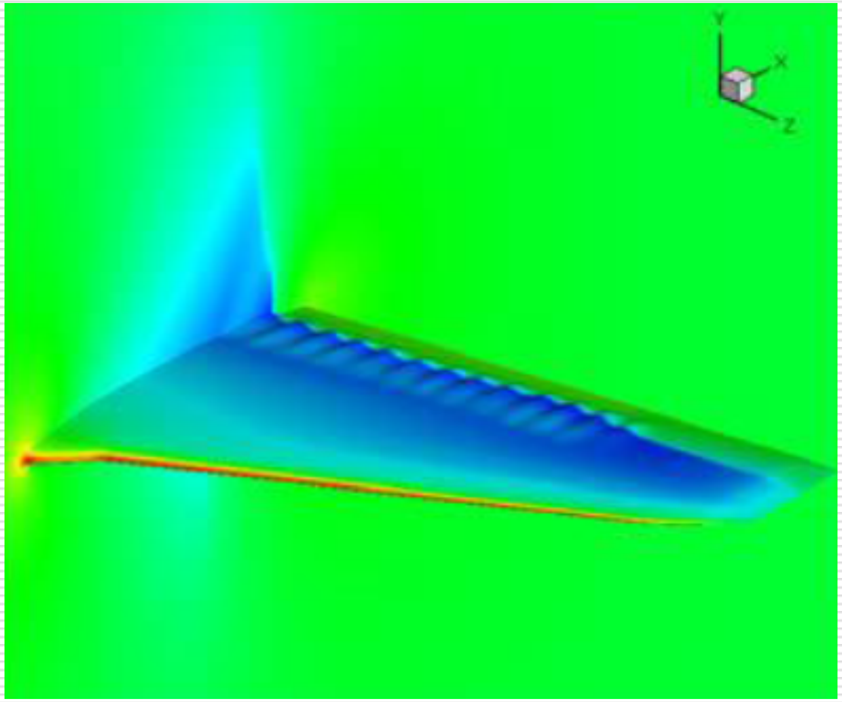

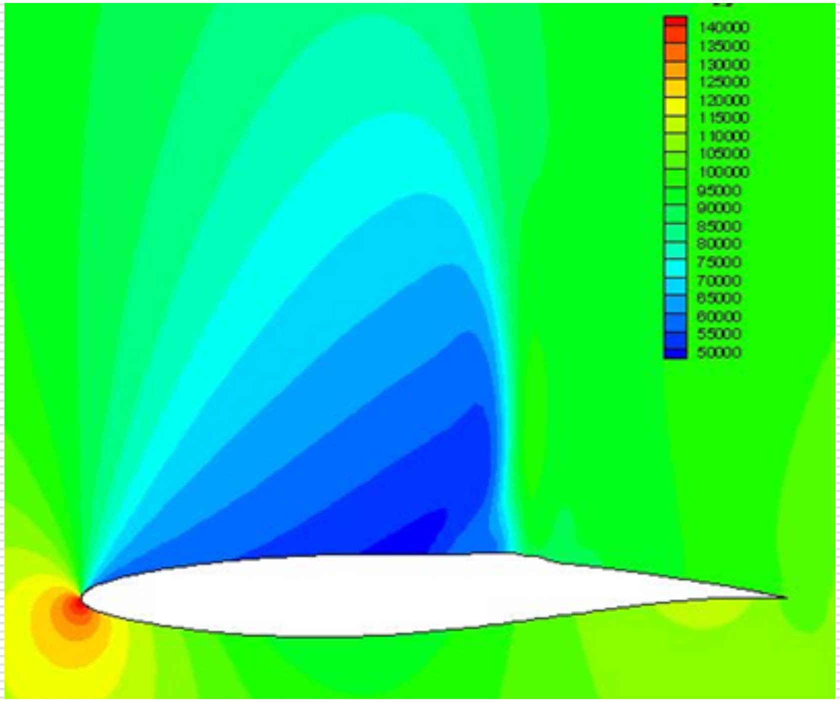

2. Flow field simulation and laminar-turbulent transition of an airfoil

- 2D finite volume structured RANS flow solver (NUAA software)
- 2D FD compressible laminar boundary layer : BL2D
- eN methodology for laminar-turbulent transition prediction : LST2D NUAA software

Flow field simulation and boundary layer solver

2D RANS

⇓

Cp outside of boundary layer

⇓

Velocity distribution outside of boundary layer with entropy correction

⇓

BL2D (Velocity profile within boundary layer)

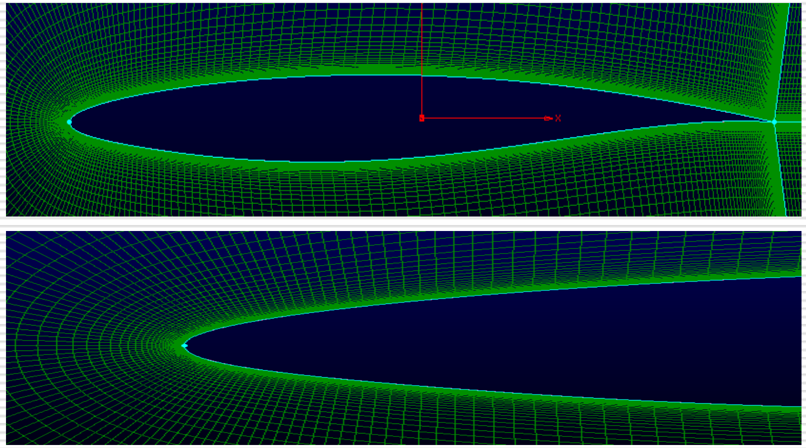

Mesh over an airfoil

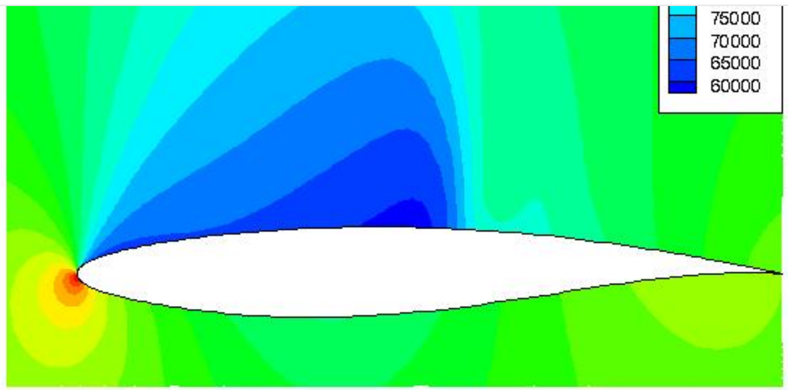

Laminar-turbulent transition on an airfoil

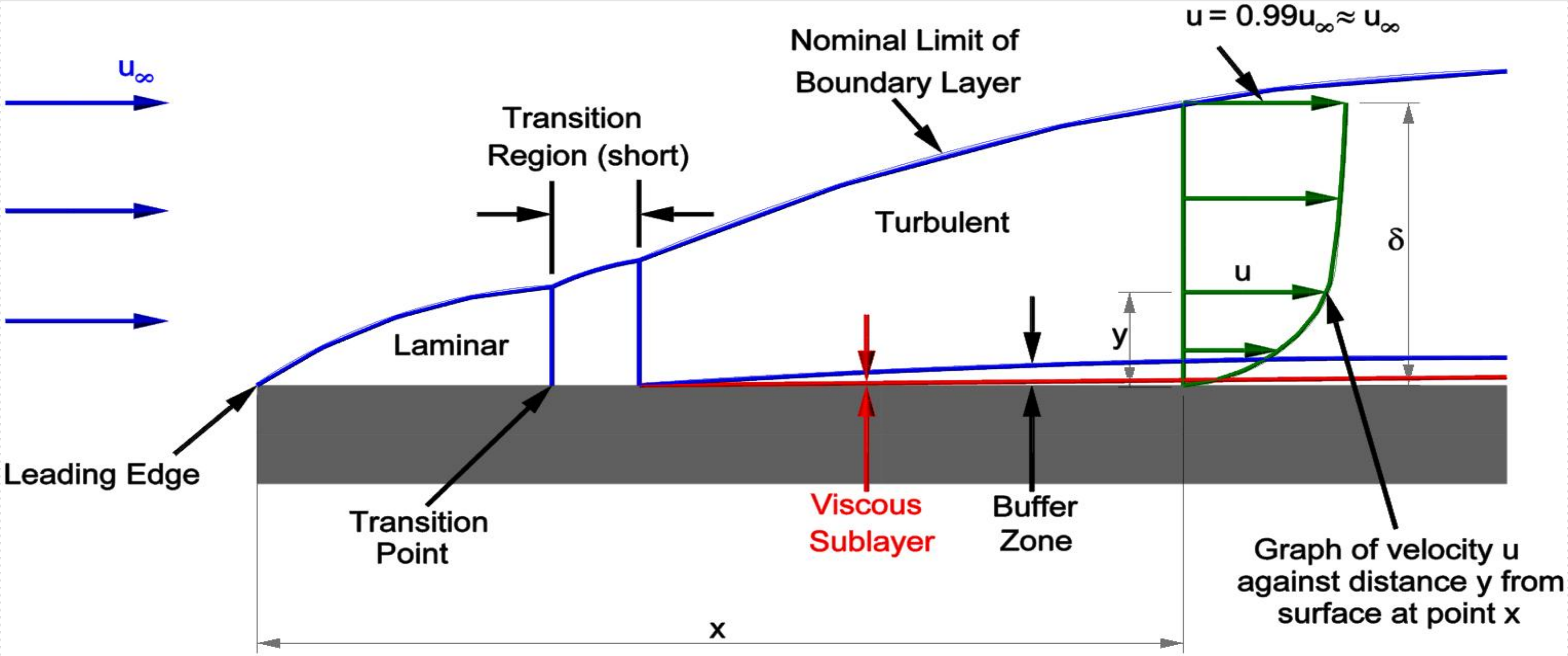

Laminar-turbulent transition on an airfoil

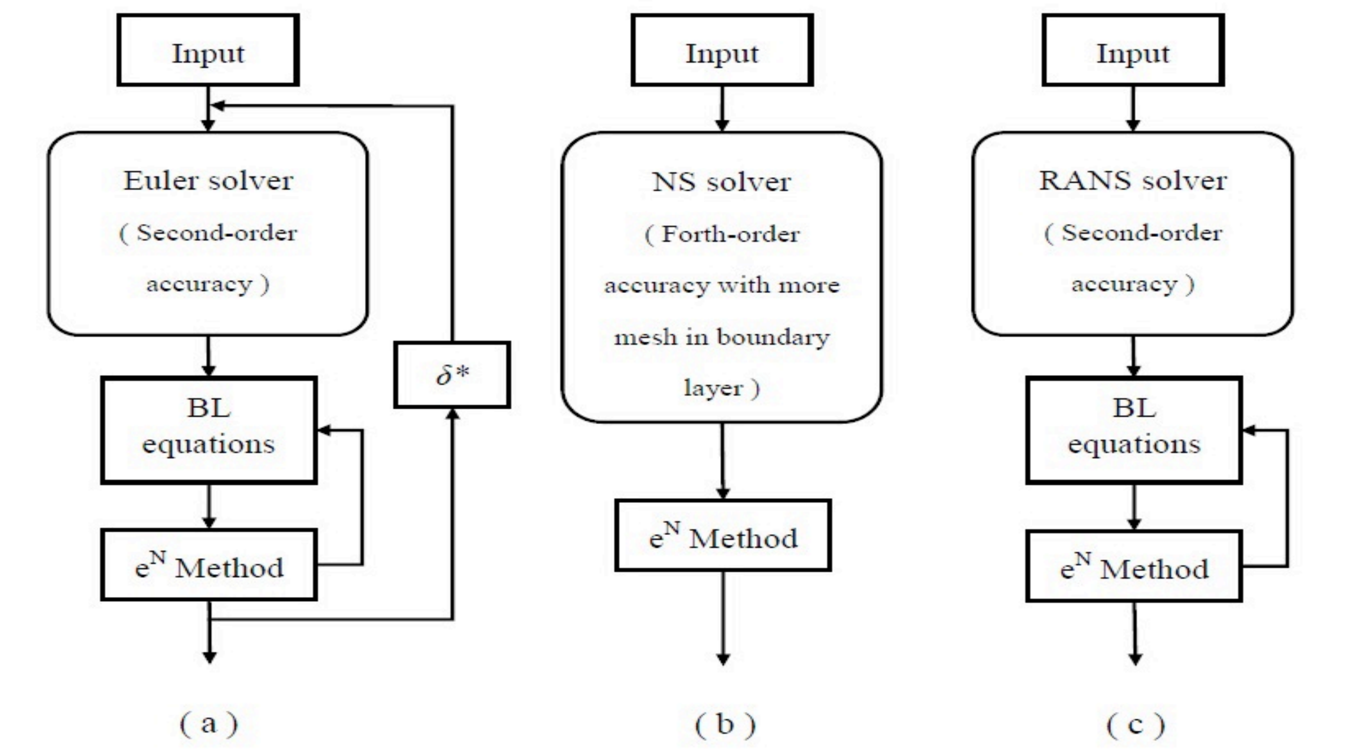

Three flow charts of the coupling between flow field solver and transition prediction

Laminar-turbulent transition on an airfoil

The computational requirements and CPU costs of three transition prediction methods.

Methods	Euler + boundary layer iteration	High-order RANS solver	Scond-order RANS solver
Numerical scheme accuracy	2nd order	4th order	2nd order
Mesh density	30,000 cells	150,000 cells	50,000 cells
Number of solver calls	≥ 6	1	1
Number of BL analysis	6×3	0	1×3
Number of e^N calls	6×3	1	1×3
CPU cost (Minutes)	2.4	≥ 5	1.3

3. Methodology for NLF airfoil shape design optimization

- NLF airfoil shape design optimization: objective functions and analysis of optimized results
- Wave drag reduction of the NLF airfoil during the shape design optimization procedure
- A mathematical formulation for the NLF airfoil shape optimization at transonic regime

Shape parameterization and search space

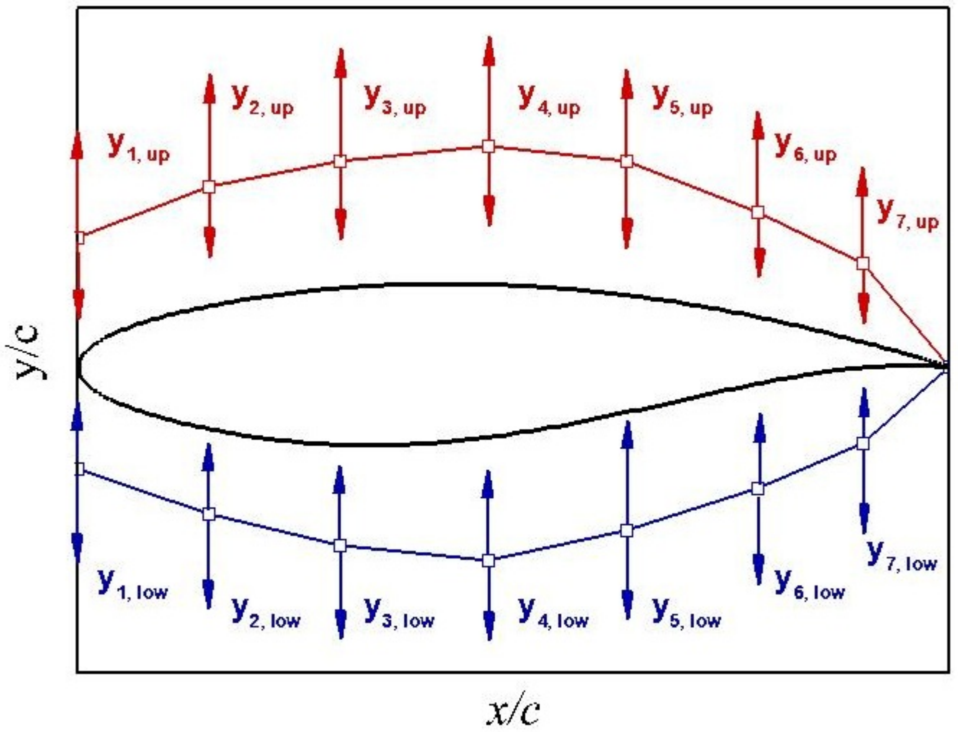

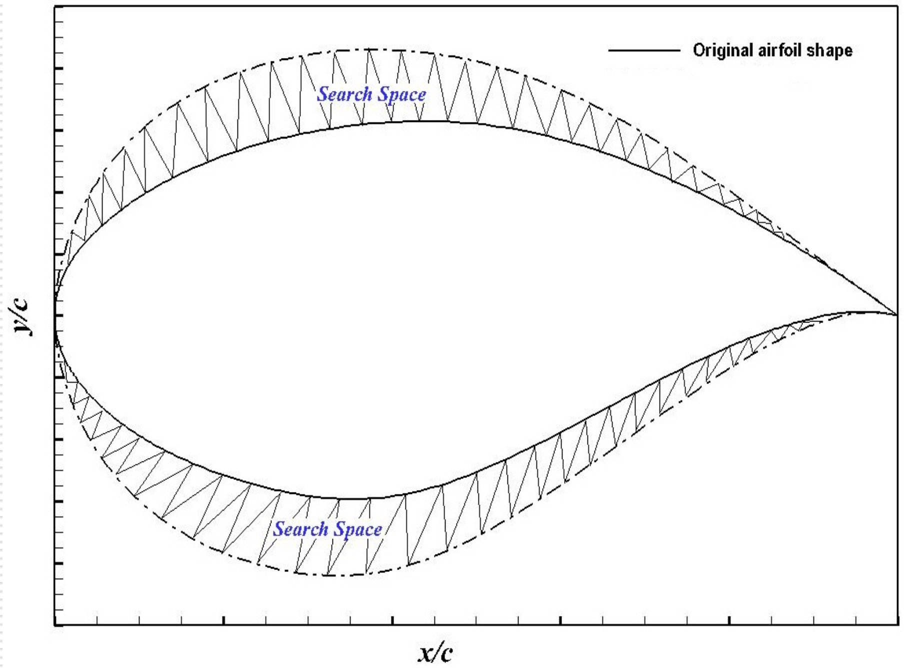

3.1 Optimization problem definition

Delay transition location to design NLF airfoil (J1) ?

or/and

Total drag minimization to design NLF airfoil (J2) ?

Delay transition J1 =

$$\begin{cases} \max\limits_{Y} \mathcal{J} = x_{upper} + x_{lower} \\ Y = (y_{1,up}, \cdots, y_{7,up}; y_{1,low}, \cdots, y_{7,low}) \end{cases}$$

Total drag minimization J2 =

$$\begin{cases} \min\limits_{Y} \mathcal{J} = C_{D\,total} \\ Y = (y_{1,up}, \cdots, y_{7,up}; y_{1,low}, \cdots, y_{7,low}) \end{cases}$$

Method 1: Total drag minimization optimization (1)

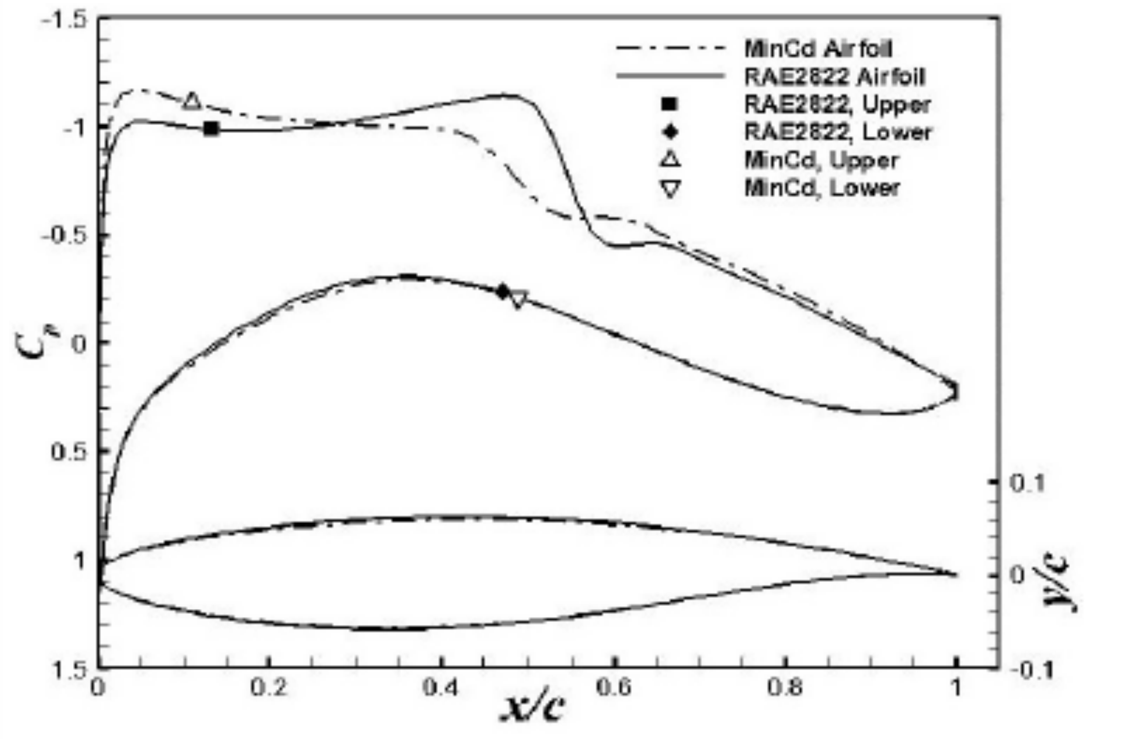

Pressure distributions, transition locations on the RAE2822 and total drag minimization airfoil.

Method 1: Total drag minimization optimization (2)

Aerodynamic performance of RAE2822 and total drag minimized airfoils (x_{upper} and x_{lower} are transition locations on upper and lower surfaces of the airfoil respectively).

	$RAE2822$ airfoil	$MinC_D$ airfoil
C_L	0.6935	0.6905
C_{Dtotal}	0.01317	0.01178
$C_{Dpressure}$	0.008207	0.006439
$C_{Dviscous}$	0.005162	0.005345
x_{upper}/c	0.1333	0.1098
x_{lower}/c	0.4699	0.4871

***Results:** the total drag minimization optimization **can** reduce the wave drag, **but it** does not delay the transition location.*

Method 2: Transition location maximization (1)

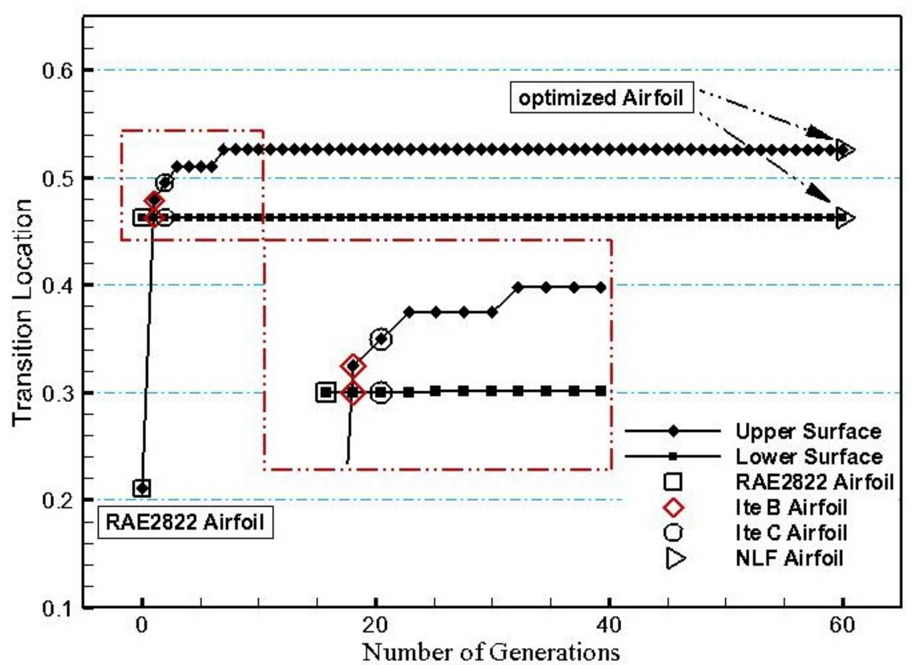

Objective function convergence history of the NLF airfoil optimization

IteB airfoil : best airfoil in second generation;

IteC airfoil : best airfoil in third generation.

The aerodynamic performance of RAE2822 and NLF airfoils.

Airfoil	$RAE2822$	$IteB$	$IteC$	NLF
C_L	0.7064	0.7114	0.7081	0.7187
$C_{D_{pressure}}$	0.008095	0.008417	0.009039	0.009403
x_{upper}/c	0.2102	0.4784	0.4943	0.5258
x_{lower}/c	0.4624	0.4627	0.4622	0.4631

Method 2: Transition location maximization (2)

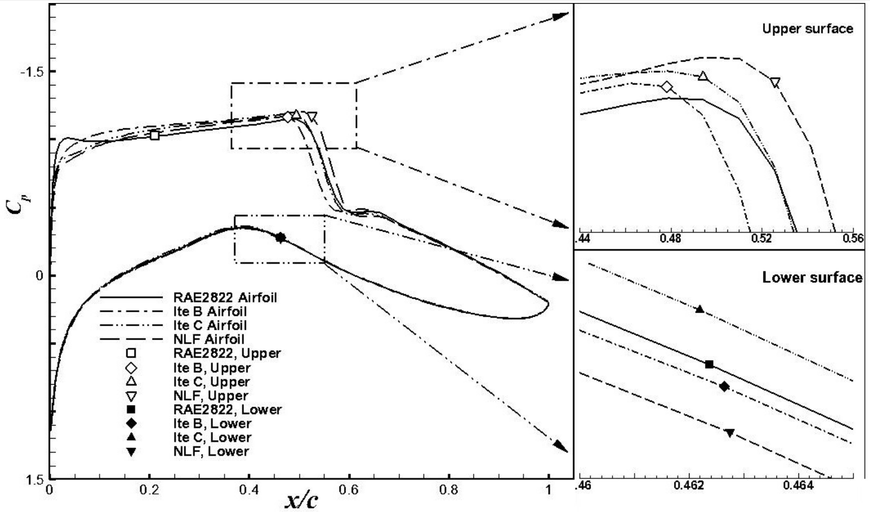

The laminar flow range increased, but the wave strength increased simultaneously !

➔ In this lecture: find a method to control the shock wave in the neighborhood of the trailing edge of airfoils ?

3.2 Wave drag reduction of the NLF airfoil during the design optimization procedure with a bump

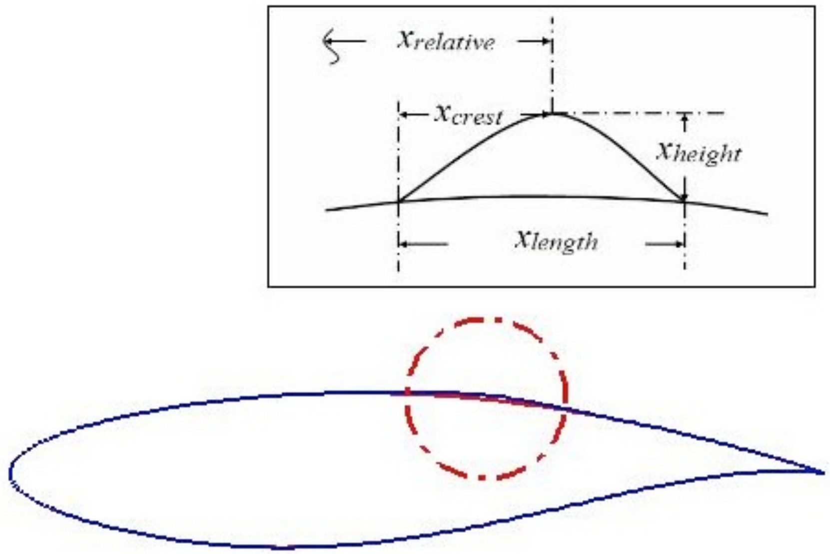

Shock wave minimization, J =

$$\begin{cases} \min\limits_{X} \mathcal{J} = C_{D_{wave}} \\ X = (x_{height}, x_{length}, x_{relative}) \end{cases}$$

3.2 Wave drag reduction of the NLF airfoil during the design optimization procedure with bump (1)

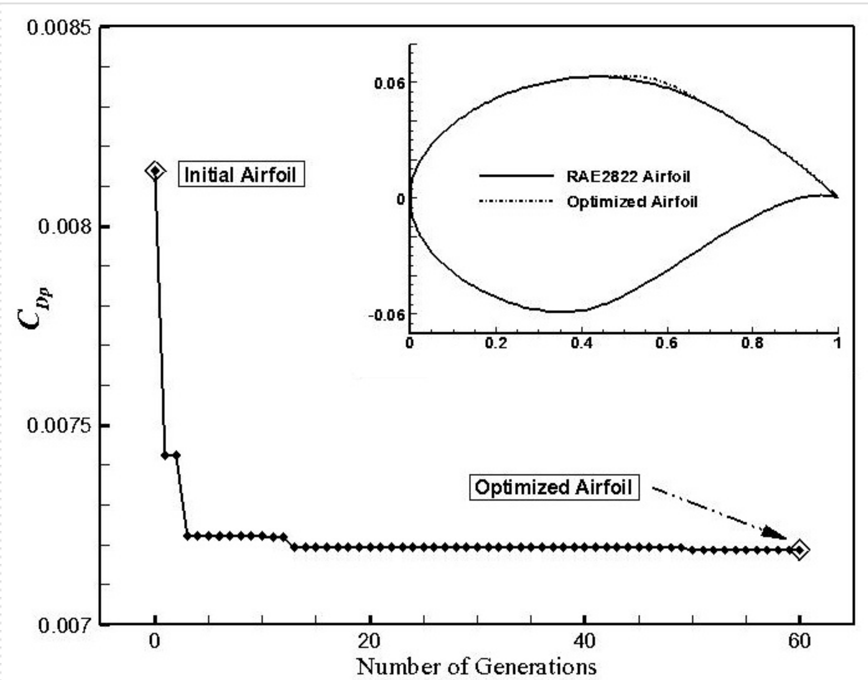

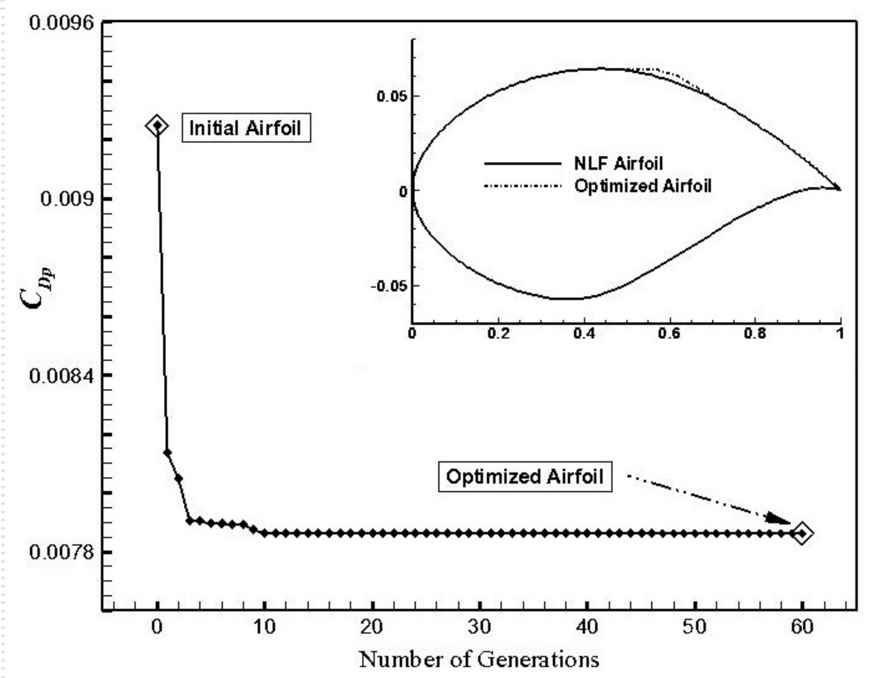

Convergence history for shape optimization of a bump installed on the RAE2822 airfoil (left) and the NLF airfoil (right).

3.2 Wave drag reduction of the NLF airfoil during the design optimization procedure with bump (2)

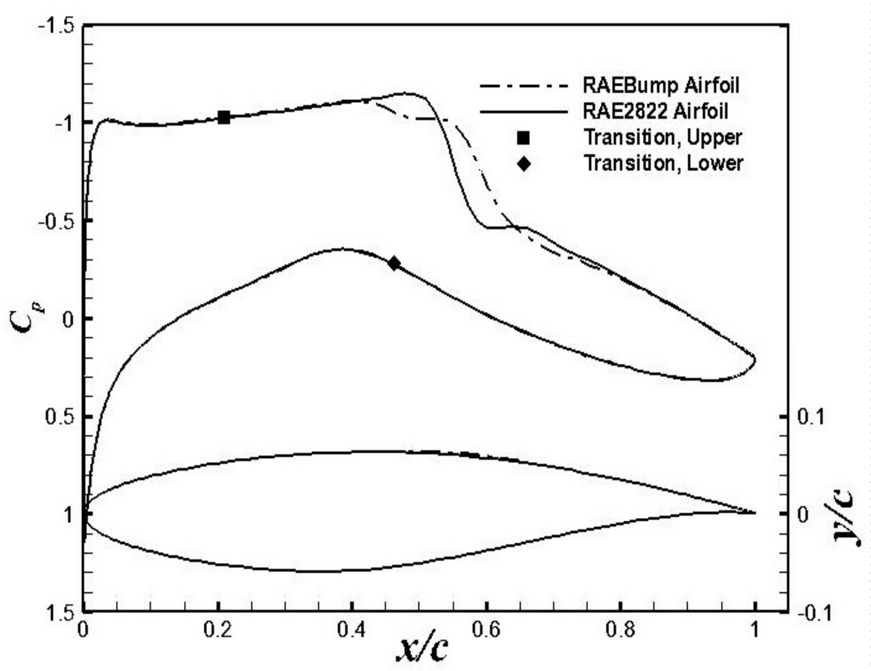

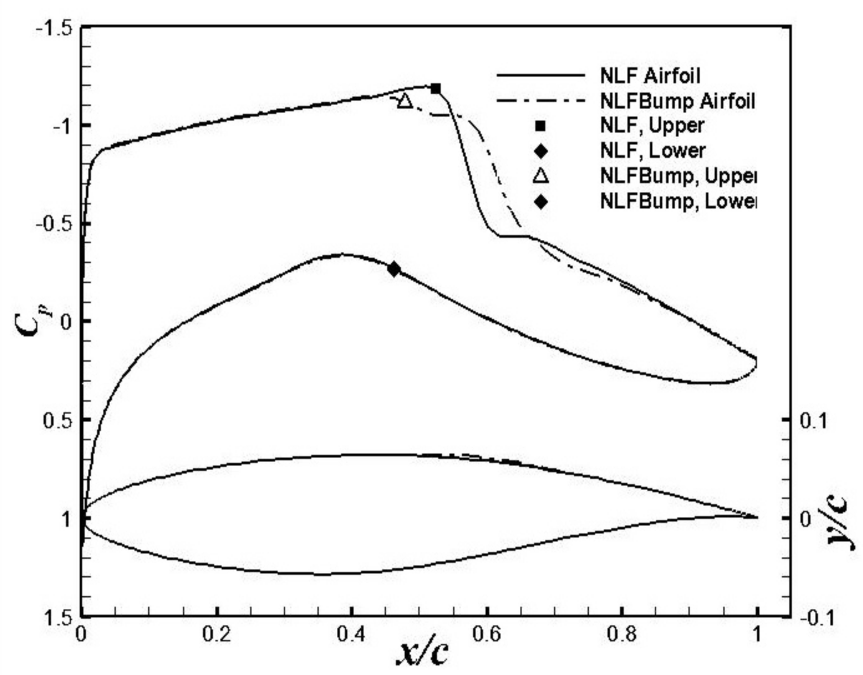

Results : Pressure distributions and transition locations on RAE2822 airfoil and airfoil equipped with a bump (left) and on NLF airfoil equipped with a bump (right).

3.2 Wave drag reduction of the NLF airfoil during the design optimization procedure with bump (3)

Aerodynamic performance of baseline and optimized airfoils.

Airfoils	$RAE2822$	$RAEBump$	NLF	$NLFBump$
C_L	0.7064	0.7168	0.7187	0.7366
C_{Dpres}	0.008095	0.007128	0.009403	0.007826
x_{upper}/c	0.2102	0.2102	0.5258	0.4790
x_{lower}/c	0.4624	0.4624	0.4631	0.4631

Above, two optimization examples indicate that the SCB does not affect the transition location of the flow, excepted when the transition occurs at the location of shock wave. Therefore, the SCB is an efficient device to be used during the NLF airfoil design optimization in order to weaken the shock intensity.

3.3 A mathematical formulation for the NLF airfoil shape optimization operating at transonic regime

In summary, the **mathematical** modeling of natural laminar **flow** airfoil design should **simultaneously** maximize the transition location and minimize/control the wave strength, i.e :

◆Delay the transition location to maintain a larger region of favorable pressure gradient on airfoil surface;

◆Install optimal SCB shape at the location of shock wave to **control** wave drag.

Two objective optimization functions, J1 and J2 =

$$\begin{cases} \max\limits_{(X,Y)} \mathcal{J}_1 = x_{upper} + x_{lower} \\ \min\limits_{(X,Y)} \mathcal{J}_2 = C_{D_{wave}} \\ X = (x_{height}, x_{length}, x_{relative}) \\ Y = (y_{1,up}, \cdots, y_{7,up}; y_{1,low}, \cdots, y_{7,low}) \end{cases}$$

3..3 A mathematical formulation for the NLF airfoil shape optimization at transonic regime : search spaces of design variables

The search space of airfoil shape (c is the chord length of an airfoil).

Parameters	Lower bound	Upper bound	Parameters	Lower bound	Upper bound
$y_{1,up}/c$	-0.002	0.002	$y_{1,low}/c$	-0.002	0.002
$y_{2,up}/c$	-0.003	0.003	$y_{2,low}/c$	-0.003	0.003
$y_{3,up}/c$	-0.005	0.005	$y_{3,low}/c$	-0.005	0.005
$y_{4,up}/c$	-0.005	0.005	$y_{4,low}/c$	-0.005	0.005
$y_{5,up}/c$	-0.005	0.005	$y_{5,low}/c$	-0.005	0.005
$y_{6,up}/c$	-0.003	0.003	$y_{6,low}/c$	-0.003	0.003
$y_{7,up}/c$	-0.003	0.003	$y_{7,low}/c$	-0.002	0.002

The search space of bump shape (c is the chord length of an airfoil).

	$x_{relative}/c$	x_{length}/c	x_{height}/c
Lower bound	-0.05	0.10	0.001
Upper bound	0.05	0.30	0.005

In following sections, an EAs hybridized with different games (cooperative Pareto game, competitive Nash game and hierarchical Stackelberg game) are implemented to solve two-objective optimization problem

Numerical implementation of the two Objective evolutionary shape optimization of NLA and SCB using hybridized game/EAs

1. Numerical implementation of a NLF airfoil shape optimization with a cooperative Pareto game and EAs

2. Numerical implementation of a NLF airfoil shape optimization with a competitive Nash game and EAs

3. Numerical implementation of a NLF airfoil shape optimization with a hierarchical Stackelberg game and EAs

CIMNE

4.1 Numerical implementation of a NLF airfoil shape optimization with a cooperative Pareto game

Considering the lift constraint, two-objective problem, J1 and J2 are defined as Maximization and Minimization Optimization problems

$$
\begin{cases}
\max\limits_{(X,Y)} \mathcal{J}_1 = (x_{upper} + x_{lower})(1 + \beta(C_L - C_{L0})/C_{L0}) \\
\min\limits_{(X,Y)} \mathcal{J}_2 = C_{D_{pres}}(1 - \beta(C_L - C_{L0})/C_{L0}) \\
subject\ \ to \quad \begin{array}{l} \beta = 0, when\ \ C_L \geq C_{L0} \\ \beta = 1, when\ \ C_L < C_{L0} \end{array} \\
X = (x_{height}, x_{length}, x_{relative}) \\
Y = (y_{1,up}, \cdots, y_{7,up}; y_{1,low}, \cdots, y_{7,low})
\end{cases}
$$

1. The baseline shape is the RAE2822 airfoil;
2. **Design flight conditions are M ∞= 0.729, AOA = 2.31° and Re = 1.28 × 10^7;**
3. A parallelized version of a Non-dominated Sorting Genetic Algorithm II (NSGA-II; K. Deb) is used;
4. NSGAII is run with a crossover probability 0.8, a mutation probability 0.1, a tournament method for selection operator and a population size 150.

5.1 Numerical implementation of a NLF airfoil shape optimization with a cooperative Pareto game (2)

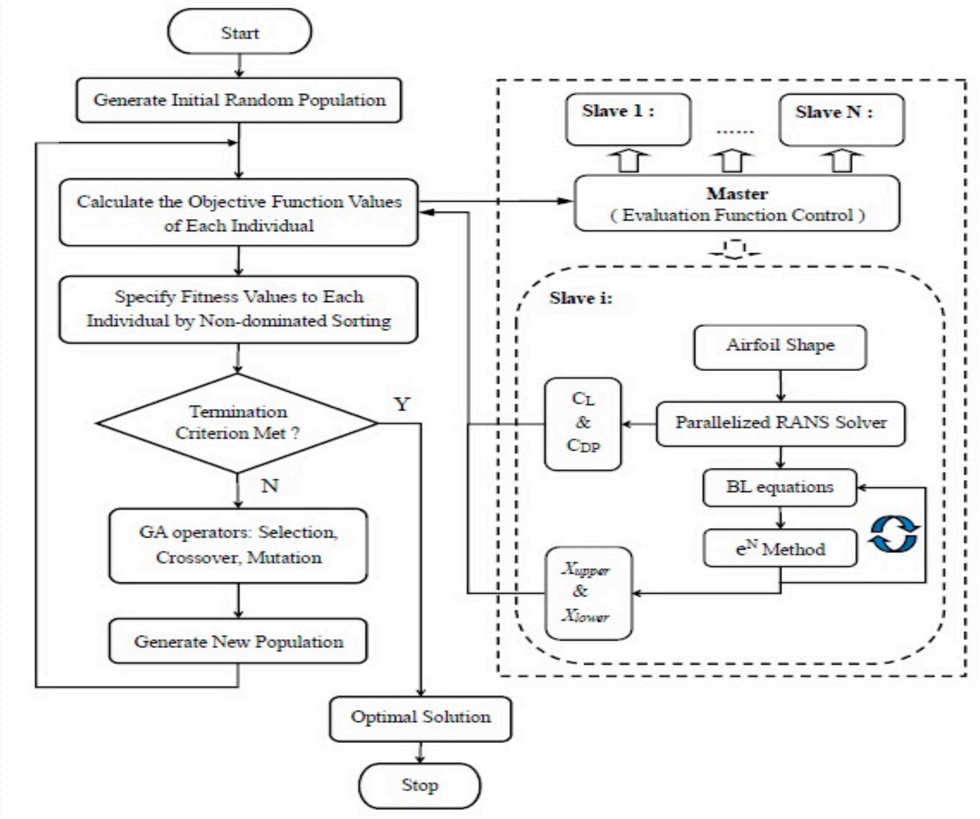

Flow chart of a parallelized NSGA-II optimization procedure for a laminar flow airfoil shape optimization.

Capture of the discontinuous Pareto Front

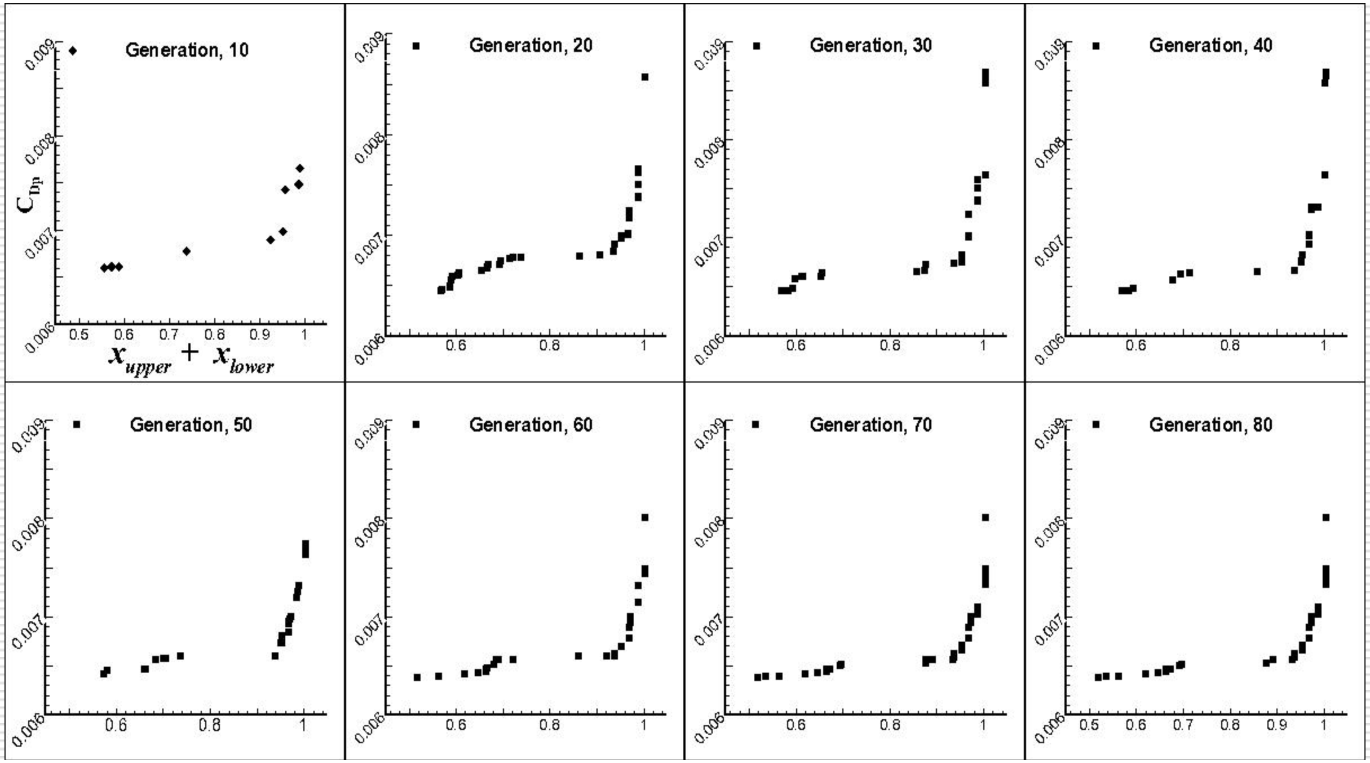

Convergence of the non-dominated solutions at different generations of the two-objective NLF airfoil shape optimization.

4.2 Numerical implementation of a NLF airfoil shape optimization with a competitive Nash game

Considering the lift constraint, two-objective problem, J1 and J2

with two players P1 (laminar) and P2 (bump wave drag)

$$\begin{cases} Player1 \begin{cases} \max\limits_{(Y)} \mathcal{J}_1(X,Y) = x_{upper} + x_{lower} \\ Subject\ \ to\ \ C_L = C_{L0} \end{cases} \\ Player2 \begin{cases} \min\limits_{(X)} \mathcal{J}_2(X,Y) = C_{D_{pres}} \\ Subject\ \ to\ \ C_L = C_{L0} \end{cases} \\ X = (x_{height}, x_{length}, x_{relative}) \\ Y = (y_{1,up}, \cdots, y_{7,up}; y_{1,low}, \cdots, y_{7,low}) \end{cases}$$

A** 3-level Parallelization of the **Nash EAs (PNEAs) is used to** solve the above **problem,

- *level-1 : **parallelization is performed on Nash players**; (symetric game)*
- ***level**-2 : **parallelization is on individuals within population;** (individuals of a population)*
- ***level**-3 : **parallelization** of **RANS solver***

4.2 Numerical implementation of a NLF airfoil shape optimization with a competitive Nash game

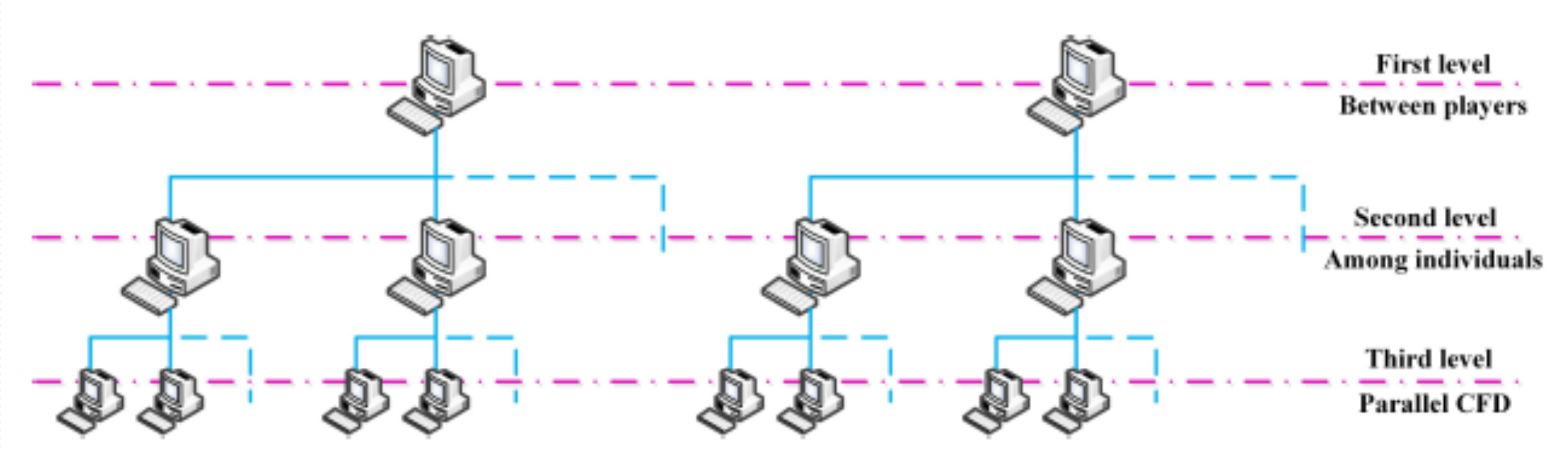

Diagram showing the three levels of parallelism implemented in Nash Evolutionary Computing.

4.3 Numerical implementation of a NLF airfoil shape optimization with a competitive Nash game

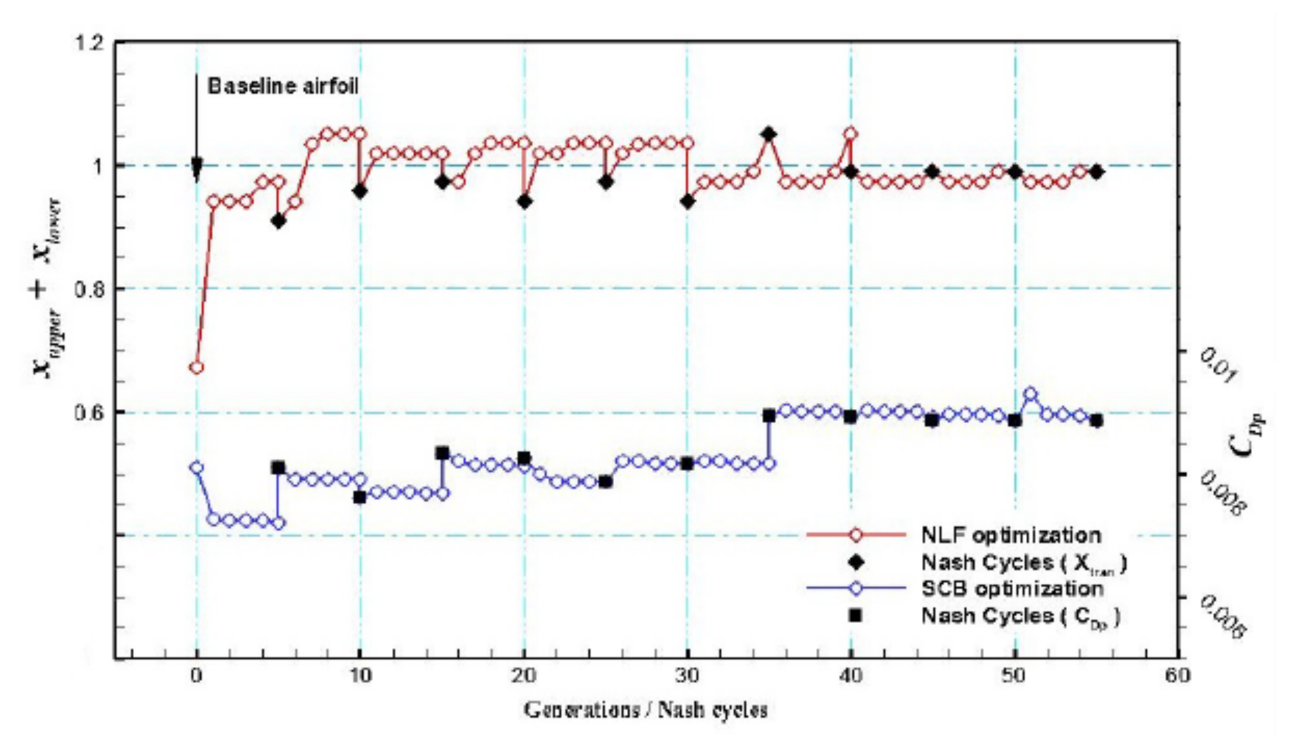

Convergence history of the Nash equilibrium.

4.4 Numerical implementation of a NLF airfoil shape optimization with a hierarchical Stackelberg game

the design territory split is kept as the same as for the above Nash game. Considering the lift constraint, the equivalent Stackelberg optimization formulation is defined as follows :

Considering the lift constraint, a two-objective problem, J1 and J2 is :

$$Leader: \begin{cases} \max\limits_{(Y)} \mathcal{J}_1(X,Y) = x_{upper} + x_{lower} \\ Subject\ \ to\ \ C_L = C_{L0} \\ X = (x_{height}, x_{length}, x_{relative}) \\ Y = (y_{1,up}, \cdots, y_{7,up}; y_{1,low}, \cdots, y_{7,low}) \end{cases}$$

$$Follower: \begin{cases} \min\limits_{(X)} \mathcal{J}_2(X,Y) = C_{D_{pres}} \\ Subject\ \ to\ \ C_L = C_{L0} \\ X = (x_{height}, x_{length}, x_{relative}) \\ Y = (y_{1,up}, \cdots, y_{7,up}; y_{1,low}, \cdots, y_{7,low}) \end{cases}$$

4.4 Numerical implementation of a NLF airfoil shape optimization with a hierarchical Stackelberg game

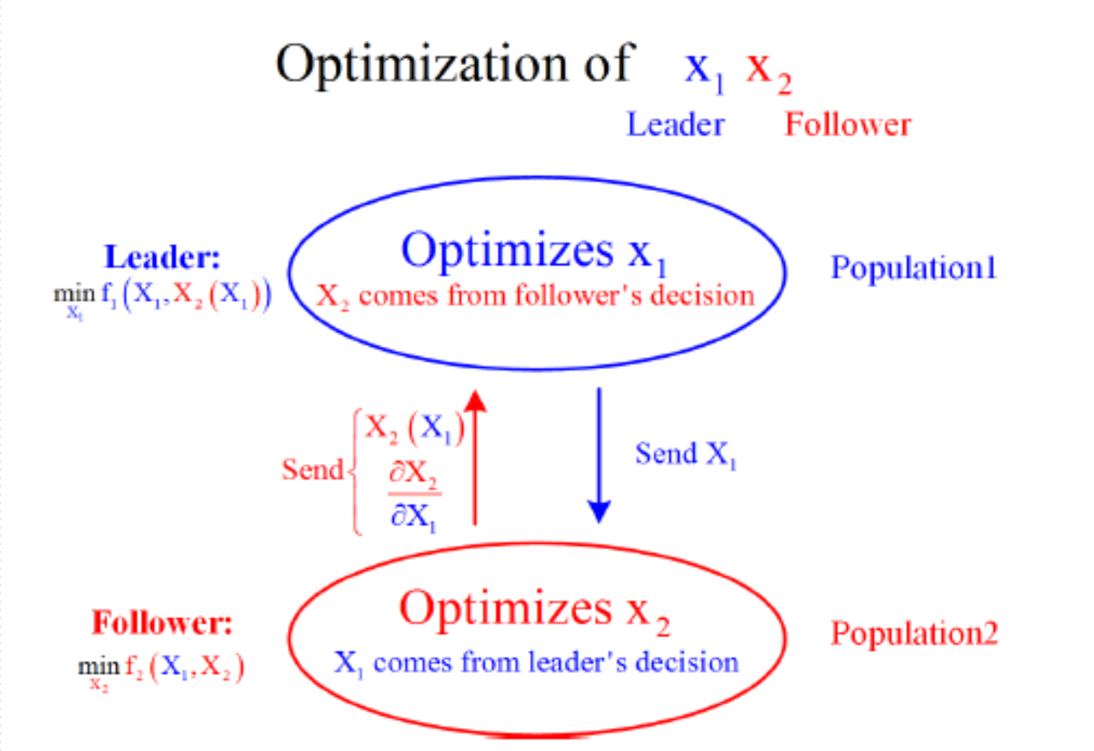

Diagram of a Stackelberg Evolutionary Algorithm.

4.3 Numerical implementation of a NLF airfoil shape optimization with a hierarchical Stackelberg game

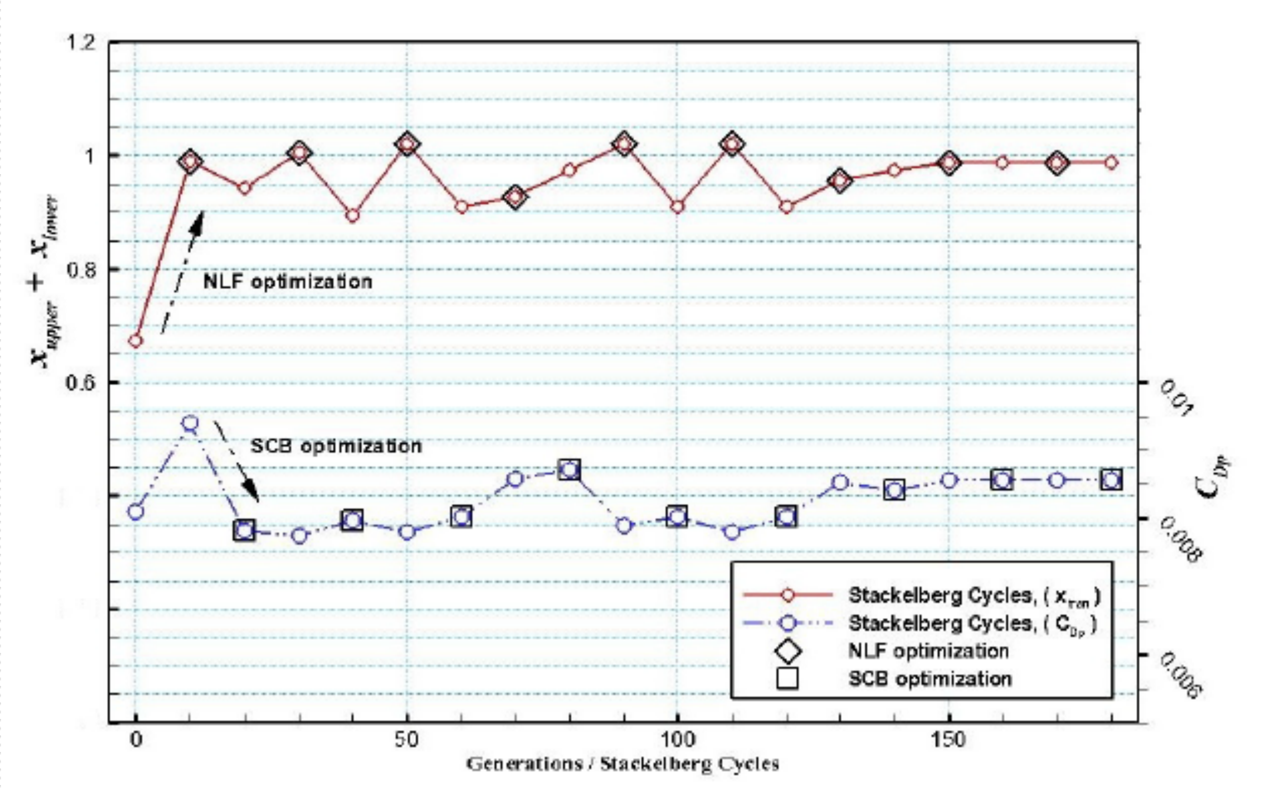

Convergence history of the Stackelberg solution.

5. Optimization： results and analysis

6.1 Optimization results with ***different*** *game strategies*

Table 1. *CPU cost for computing Pareto front,Nash and Stackelberg equilibria*

	Pareto front	Nash equilirium	Stackelberg
Number of parameters	17(14+3)	14/3	14/3
Population size	150	150/50	150/50
Generations	80	$9 \times (5/5)$	$9 \times (10/10)$
Crossover probability	0.8	0.8	0.8
Mutation probability	0.1	0.1	0.1
Number of cores	256	256	256
CPU performance	CPU E5-2640	CPU E5-2640	CPU E5-2640
CPU cost(h)	140	90.25	180.5

The aerodynamic performances of selected Pareto Members A, B, C, RAE2822, RAEBump, NLF, NLFBump , NE and SE airfoils are presented on Tables 1-3. It shows that the shock wave intensity decreases obviously by installing the bump. Positions of the NE and SE with Pareto front in the solution space is shown in Figure 1. It can be observed that the transition of NE and SE are delayed, by 51.07% and 47.84% of chord length on the upper airfoil respectively. Moreover, the shock wave intensity does not increase when compared with that of the baseline shape.

5.1 Optimization results with the three game strategies

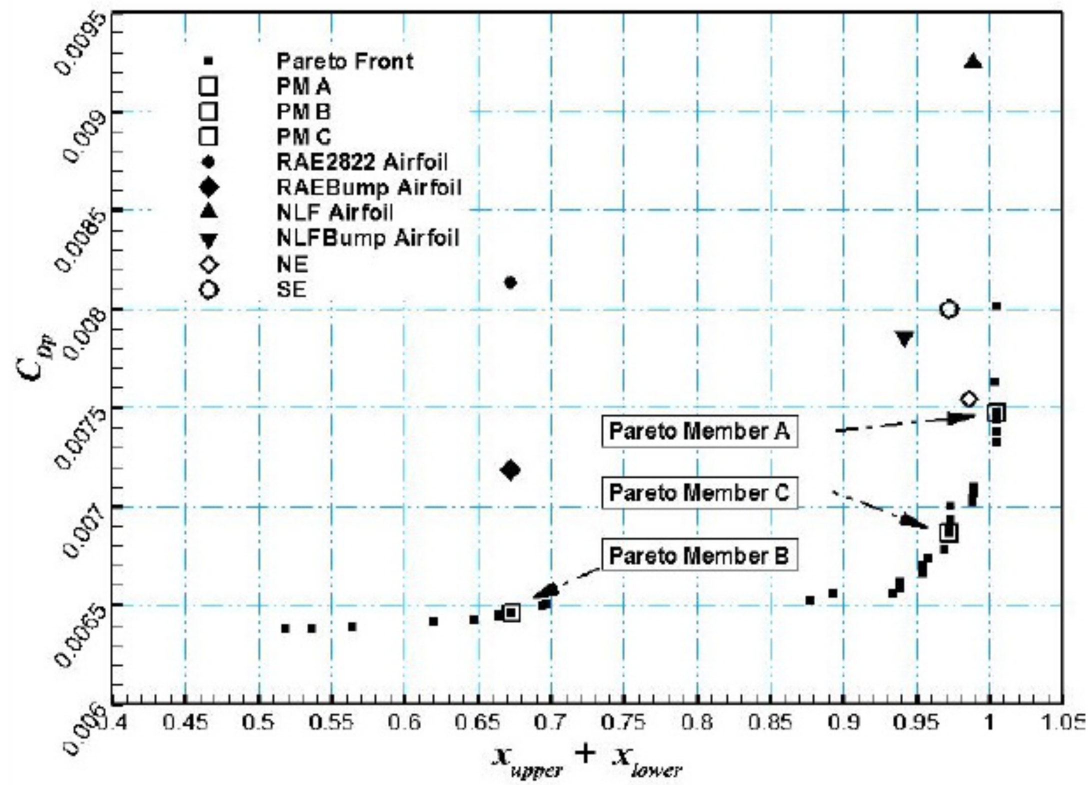

Fig.1 Converged Pareto front and solutions of NE, SE, RAEBump, NLF, NLFBump and Baseline shape.

6.1 Optimized results with game strategies : quality comparisons

Table 2. *Aerodynamic performances of airfoils*
(Calculated with transition prediction simulation)

Airfoils	x_{upper}/c	x_{lower}/c	C_L	C_{Dpres}	C_{Dvis}	C_{Dtotal}	$M \cdot L/D$
RAE2822	0.2102	0.4624	0.7064	0.008095	0.003179	0.01127	45.69
RAEBump	0.2102	0.4624	0.7168	0.007128	0.003178	0.01031	50.70
NLF	0.5258	0.4631	0.7187	0.009403	0.002713	0.01212	43.24
NLFBump	0.4790	0.4631	0.7366	0.007826	0.002779	0.01061	50.63
NE	0.5107	0.4786	0.7040	0.007519	0.002727	0.01024	50.12
SE	0.4784	0.4780	0.7084	0.008000	0.002794	0.01079	47.86
PM A	0.5416	0.4630	0.7181	0.007428	0.002647	0.01008	51.88
PM B	0.2166	0.4630	0.7016	0.006358	0.003217	0.009575	53.41
PM C	0.5104	0.4628	0.7056	0.006859	0.002724	0.009583	53.67

Table 3. *Aerodynamic performances of airfoils (calculated with full turbulence simulation).*

Airfoils	C_L	C_{Dpres}	C_{Dvis}	C_{Dtotal}	$M \cdot L/D$
RAE2822	0.7064	0.008095	0.005585	0.01368	37.64
RAEBump	0.7168	0.007128	0.005602	0.01273	41.05
NLF	0.7187	0.009403	0.005547	0.01495	35.05
NLFBump	0.7366	0.007826	0.005584	0.01341	40.04
NE	0.7040	0.007519	0.005640	0.01316	39.00
SE	0.7084	0.008000	0.005570	0.01357	38.06
PM A	0.7181	0.007428	0.005592	0.01302	40.20
PM B	0.7016	0.006358	0.005642	0.01200	42.62
PM C	0.7056	0.006859	0.005621	0.01248	41.21

Appendix

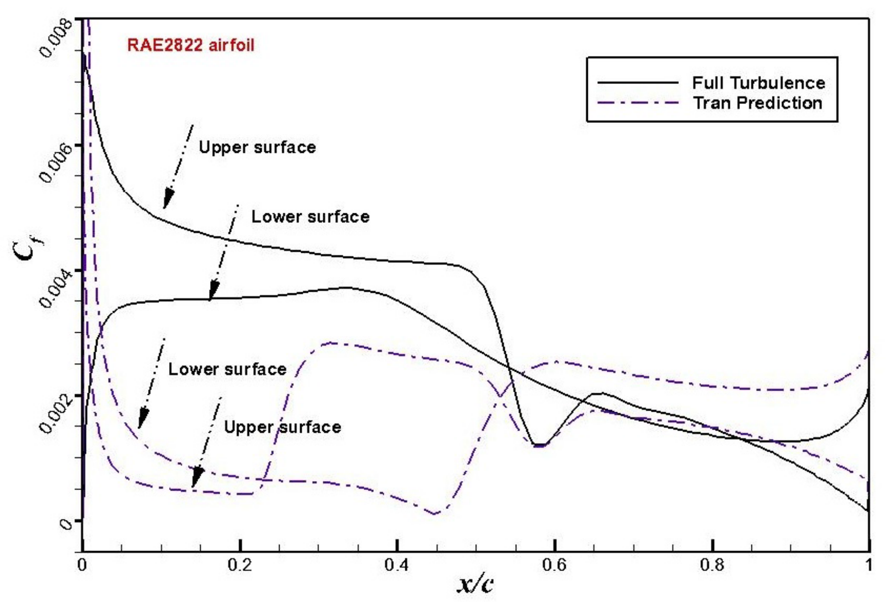

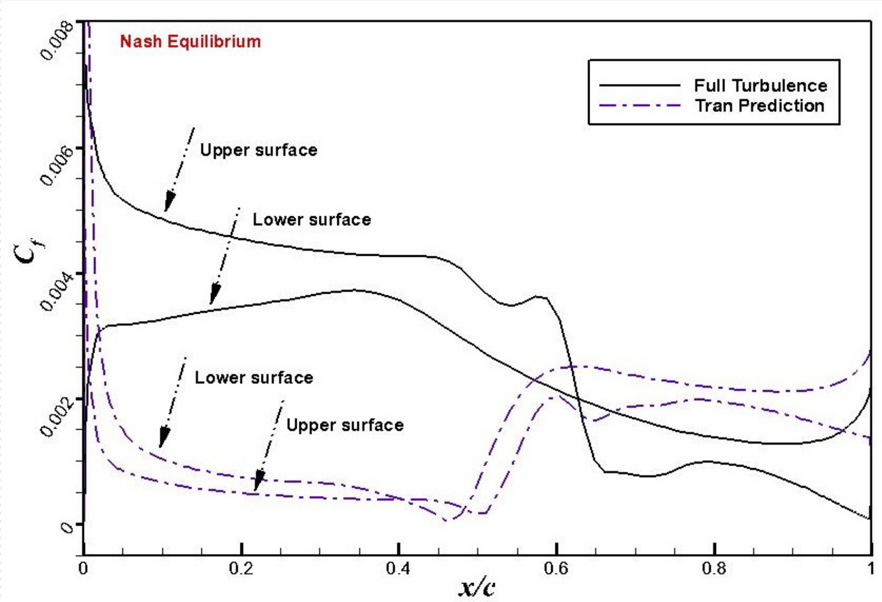

Comparison of skin friction coeffcient distributions between full turbulence simulation and simulation with transition prediction on

i) the baseline shape (**left**)

ii) the Nash equilibrium solution (**right**).

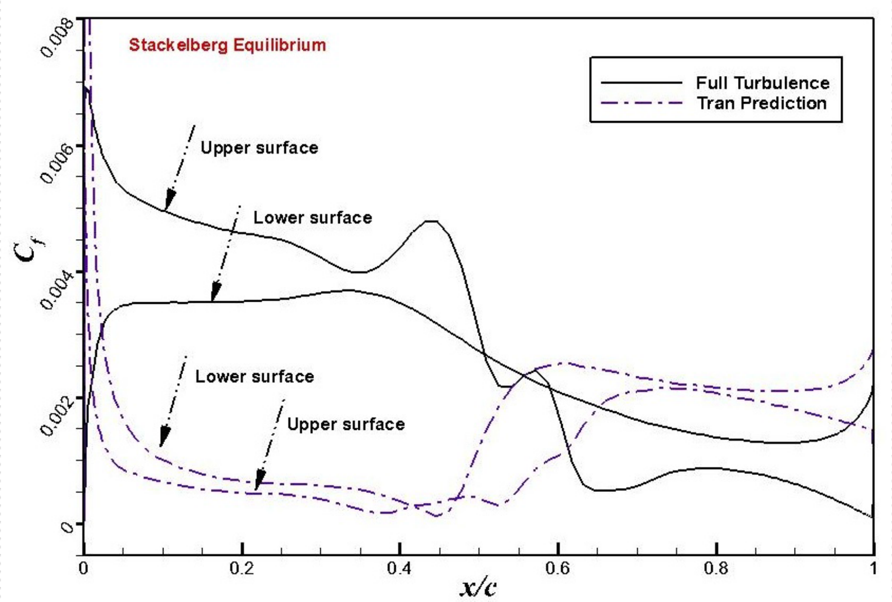

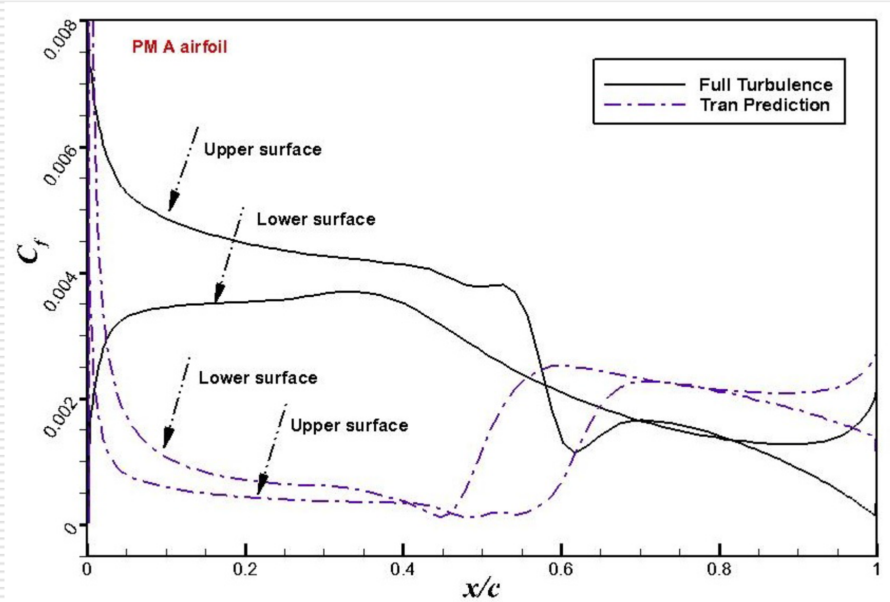

Comparison of skin friction coeffcient distributions between full turbulence simulation and simulation with transition prediction on

- **the Stackelberg equilibrium** (left) **solution**
- Pareto Member A (PMA) airfoil (right)selected from Pareto front.

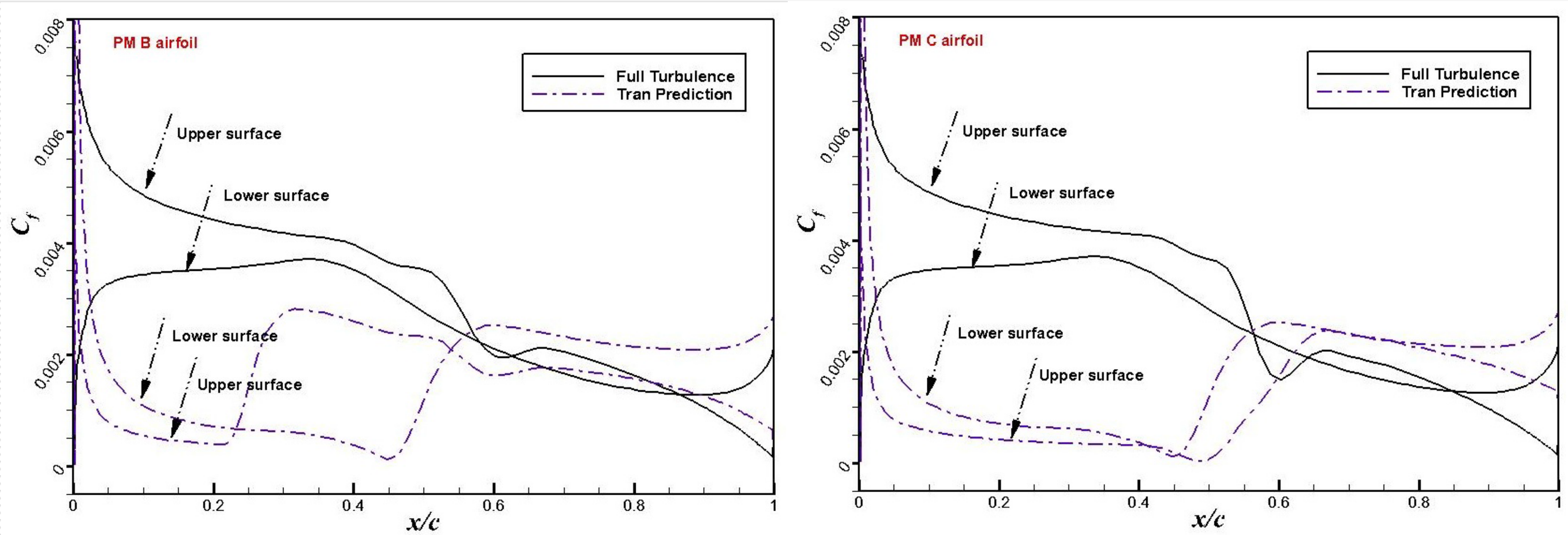

Comparison of skin friction coeffcient distributions between full turbulence simulation and simulation with transition prediction on the PM B airfoil (left) and PM C airfoil (right) selected from Pareto front.

6.2 Discussion of the influence of the territory split location in game strategies with respect to flow physics

- **Consider** the non-physical Nash solution and compare it with the physical Nash equilibrium solution:

$$Physical\ \ Nash: \begin{cases} \max\limits_{(Airfoil)} \mathcal{J}_1 = x_{upper} + x_{lower} \\ \min\limits_{(SCB)} \mathcal{J}_2 = C_{D_{wave}} \end{cases}$$

$$Nonphysical\ \ Nash: \begin{cases} \max\limits_{(SCB)} \mathcal{J}_1 = x_{upper} + x_{lower} \\ \min\limits_{(Airfoil)} \mathcal{J}_2 = C_{D_{wave}} \end{cases}$$

6.3 Discussion of territory split in game strategies with respect to flow physics

- **Consider** the non-physical **Stackelberg** solution and compare it with the physical **Stackelberg** equilibrium solution:

$$Physical\ \ Stackelberg: \begin{cases} Leader: & \max\limits_{(Airfoil)} \ \mathcal{J}_1 = x_{upper} + x_{lower} \\ Follower: & \min\limits_{(SCB)} \ \mathcal{J}_2 = C_{D_{wave}} \end{cases}$$

$$Nonphysical\ \ Stackelberg: \begin{cases} Leader: & \max\limits_{(SCB)} \ \mathcal{J}_1 = x_{upper} + x_{lower} \\ Follower: & \min\limits_{(Airfoil)} \ \mathcal{J}_2 = C_{D_{wave}} \end{cases}$$

6.2 Analysis: territory split in game strategies with respect to flow physics

Procedure of non-physical Nash cycles.

Number of Nash cycle	C_L	x_{upper}/c	x_{lower}/c	$C_{D_{pres}}$
0	0.7064	0.2102	0.4624	0.008095
1	0.6656	0.1197	0.4626	0.007730
2	0.6832	0.1048	0.4629	0.008185
3	0.6809	0.0912	0.4626	0.008184
4	0.7022	0.0949	0.4626	0.006440
5	0.6827	0.1034	0.4631	0.007520
6	0.6780	0.08241	0.4627	0.008070
7	0.7174	0.09871	0.4631	0.006851
8	0.7000	0.07548	0.4630	0.006540

Aerodynamic performances of Nash equilibrium using non-physical Split territory.

Airfoils	C_L	x_{upper}/c	x_{lower}/c	$C_{D_{pres}}$
RAE2822	0.7064	0.2102	0.4624	0.008095
NE	0.7040	0.5107	0.4786	0.007520
Non-physical Nash	0.7000	0.07548	0.4630	0.006540

6.4 Discussion of territory split in game strategies **with respect to flow** physics

Procedure of non-physical Stackelberg cycles.

Number of Nash cycle	C_L	x_{upper}/c	x_{lower}/c	$C_{D pres}$
1	0.7064	0.2102	0.4624	0.008095
2	0.7068	0.2102	0.4624	0.008095
3	0.6781	0.2102	0.4624	0.009176
4	0.6662	0.0946	0.4629	0.007956
5	0.6933	0.1019	0.4629	0.007118
6	0.6999	0.09670	0.4628	0.006864
7	0.7100	0.1073	0.4628	0.006612
8	0.7013	0.1024	0.4628	0.006467
9	0.6996	0.1025	0.4628	0.006875
10	0.7010	0.2064	0.4622	0.006599
11	0.7032	0.2120	0.4622	0.006720
12	0.7010	0.1970	0.4624	0.006567

Aerodynamic performances of Stackelberg equilibrium ***using*** *non-physical split territory.*

Airfoils	C_L	x_{upper}/c	x_{lower}/c	$C_{D pres}$
RAE2822	0.7064	0.2102	0.4624	0.008095
SE	0.7068	0.4784	0.4780	0.007940
Non-physical Stackelberg	0.7010	0.1970	0.4624	0.006567

7. Conclusion and Perspectives (1)

Conclusion:

Based on the mathematical formulation of a NLF shape optimization problem operating at transonic regimes , an EAs hybridized with different games (*cooperative Pareto game, competitive Nash game and hierarchical Stackelberg game*) has been implemented to optimize the airfoil shape targeting a larger laminar flow region and a weaker shock wave drag simultaneously.

Each game provides different solutions with different performances. Numerical experiments demonstrate that each game coupled to the EAs optimizer can easily capture either a Pareto Front, a Nash Equilibrium or a Stackelberg solution of the two-objective shape optimization problem.

7. Conclusion and perspectives : ¡ HPC demand ! (2)

- From obtained numerical experiments , it is noticed **that one important concern related with the multi-disciplinary shape optimization in** aerodynamics **is the high** computational effort **demand.**

  - ***parallelization of the game strategy,***
  - *Parallelization of the multi disciplinary analyzer software*
  - *parallelization of each physical discipline .*

7. Conclusion and perspectives (3)

Solutions on Pareto front provide the best set of laminar flow airfoils with significantly improved aerodynamic performances. From the results it can be concluded that the **NLF** shape design optimization method coupled with games implemented in this paper is feasible and effective.

Perspectives:

- **The methodology developed in this paper can be easily extended to 3-D NLF wings or even to NLF complete aircraft shape optimization (such as** ***future Blended Wing Body (BWB)*** configurations with distributed propulsion) using **large HPC environments.**
- *Coalition games* , associated to disciplines like *aerodynamics, structure, weight, stability, noise and control*, will be considered for multi disciplinary NLF shape optimization.

8. References

[1] J. E. Green, Laminar flow control-back to future [R]. AIAA-2008-3738, 2008.

[2] J. Reneaux, Overview on drag reduction technologies for civil transport aircraft[C]// European Congress on Computational Methods in Applied Sciences and Engineering. France: ONERA, Aerodynamics Department, 2004: 2-13.

[3] S. Peter, An aerodynamic design method for supersonic natural laminar flow aircraft[D]. Standford: Department of Aeronautics and Astronautics, 2004.

[4] Jen D L, A Jameson, Natural-laminar-flow airfoil and wing design by adjoint method and automatic transition prediction[R]. AIAA-2009-897, 2009. J Driver, D W Zingg. Optimized natural-laminar-flow airfoils [J]. AIAA Journal, 2002, 40(6): 4-6.

[5] Z.L. Tang, J. Periaux, Constraint Handling in Adjoint/Nash Optimization Strategy for Multi-Criteria Aerodynamic Design, Computer Methods in Applied Mechanics and Engineering, 271 (2014) pp: 130-143.

[6] J. Periaux, F. Gonzalez, D.S. C. Lee, Evolutionary Optimization and Games Strategies for Advanced Design: Applications to Aeronautics, Springer, May 2015

[7] D.S. Lee, G. Bugeda , J. Periaux, E. Onate, Robust active shock control bump design optimisation using hybrid parallel MOGA, Elsevier , Computers & Fluids 80 (2013) 214–224

Application 2

Multidisciplinary shape design optimization of air-vehicle with distributed propulsion

Z.L. Tang, D.H. Yang, J. Periaux

A lecture to be presented at Stanford Univ. (Dept A&A)
next August !

Background

Layout characteristics of blended wing body

- The total weight of take-off is reduced by 15%
- Oil consumption per mile per se is reduced by 27%
- Empty weight reduction by 12%
- Lift to drag ratio increased by 2
- Greatly reduce the noise of fligh

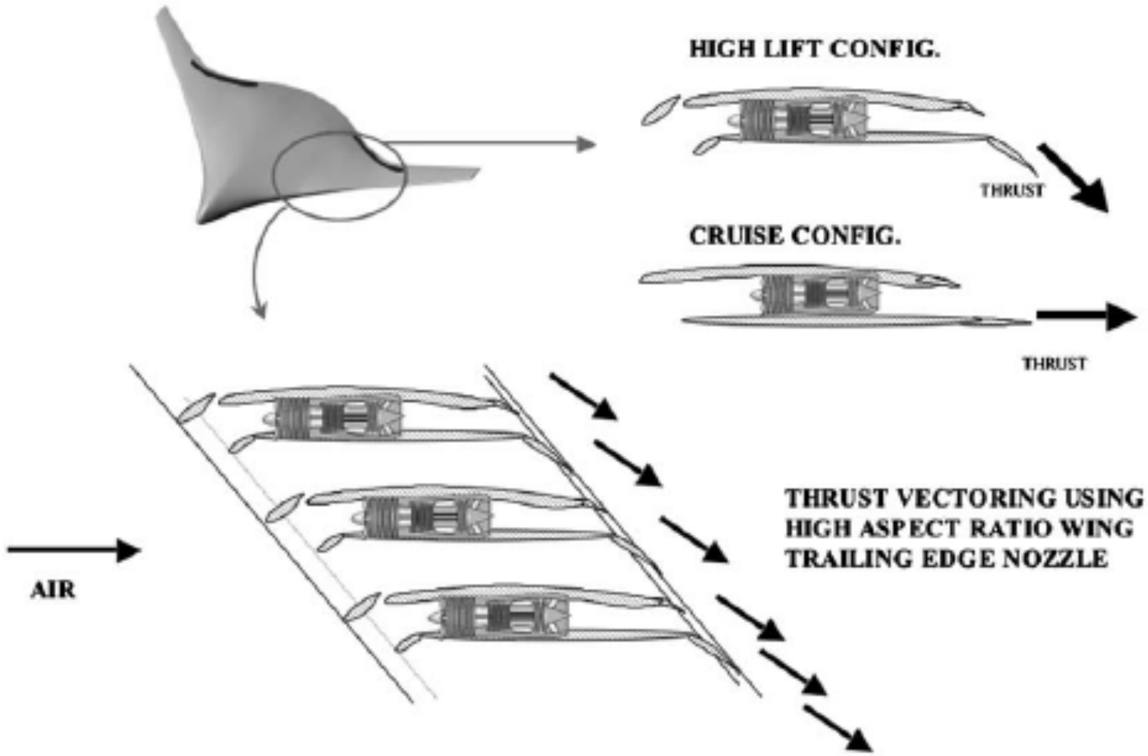

Distributed engines embedded in blended wing body aircraft

Distributed propulsion BWB aircraft with boundary layer ingestion

Bakground

1.2 Why to design distributed propulsion vehicle

Compared with the traditional vehicle, the distributed propulsion air-vehicle obviously has the following advantages. :

- **Reduce the high performance requirements of the engine**
- **Reduce aircraft noise**
- **Improve the efficiency of thrust**
- **Improve flight performance and improve safety**
- **Reduce the lift induced drag**
- **Reduce wing load and therefore its weight**
- **Improve aircraft stability and control ability**
- **Reduce the area and weight of the rudder**
- **Improve the safety and reliability of the propulsion system**
- **Short takeoff and landing range**
- **BLI can increase fuel efficiency and increase flight range further.**

CIMNE

Background

The current status of distribution propulsion vehicle

L. Leifsson selected two BWB aircrafts as design platform.

- **BWB aircraft with conventional propulsion (Installed 4 large turbofan engines with pylons)**
- **Distributed propulsion BWB aircraft (installing 8 engines with boundary layer ingestion)**

The effects of distributed propulsion on flight performance and weight are studied by means of multidisciplinary optimization.

Results indicate:

- **More than 2/3 of energy consumption is saved**
- **Gust load and flutter are reduced**
- **Wing weight is reduced significant**

CIMNE

Shape design and MDO of air-vehicles with distributed propulsion

2.1object of study

Cost functions

- Takeoff weight minimization
- Fuel consumption rate minimization
- Lift/Drag maximization

Constraints

- Flight control
- Flight range
- Cabin volume

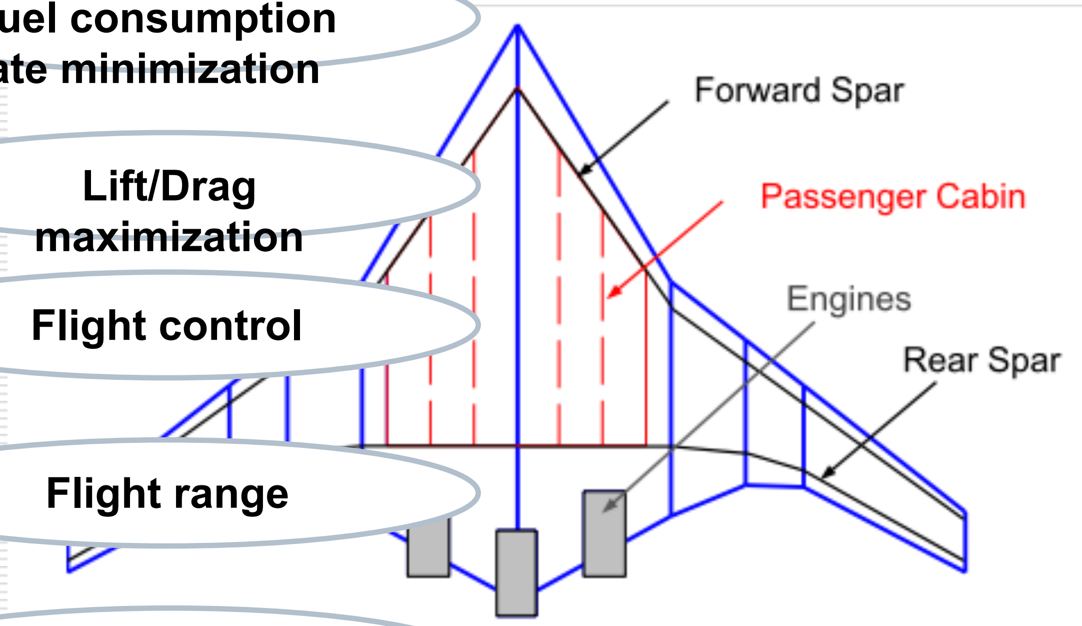

Design variables

Variables		Reference value
b	Spanwise length	80.0
η_2	Spanwise position of 2nd section	0.433
C_1	Chord length of section 1	42.0
C_2	Chord length of section 2	12.0
C_3	Chord length of section 3	3.33
t_1	Thickness of section 1	5.0862
t_2	Thickness of section2	1.4532
t_3	Thickness of section 3	0.404
X_{le}	Front position of crabin	2.0
L_{cabin}	Length of carbin	28.0
Λ_1	Swept angle 1	50.0
Λ_2	Swept angle 2	30.0
H_{cruise}	Flight altitude	12000
W_{fuel}	Fuel weight	158757.7
T_{sls}	Maximum static thrust of sea level	113429.6

Design conditions

参数		数值
M	Mach number at cruise	0.85
N_{eng}	Number of engines	4-8
N_{pass}	Number of passengers	480
R	Flight range (miles)	7700
W_d	Pipe weight factor	0.05

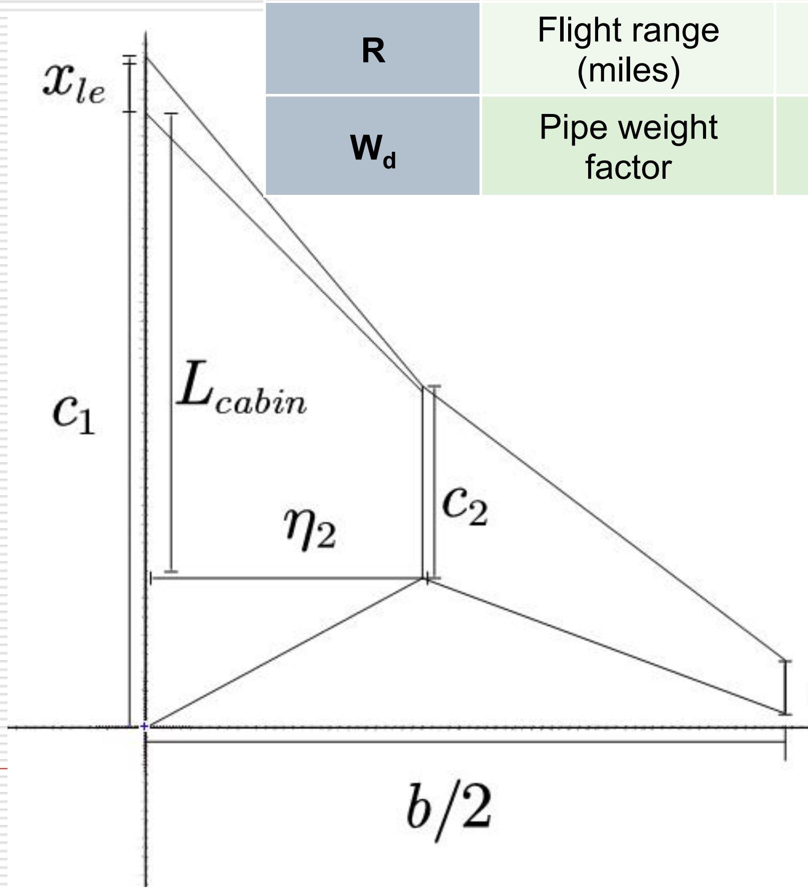

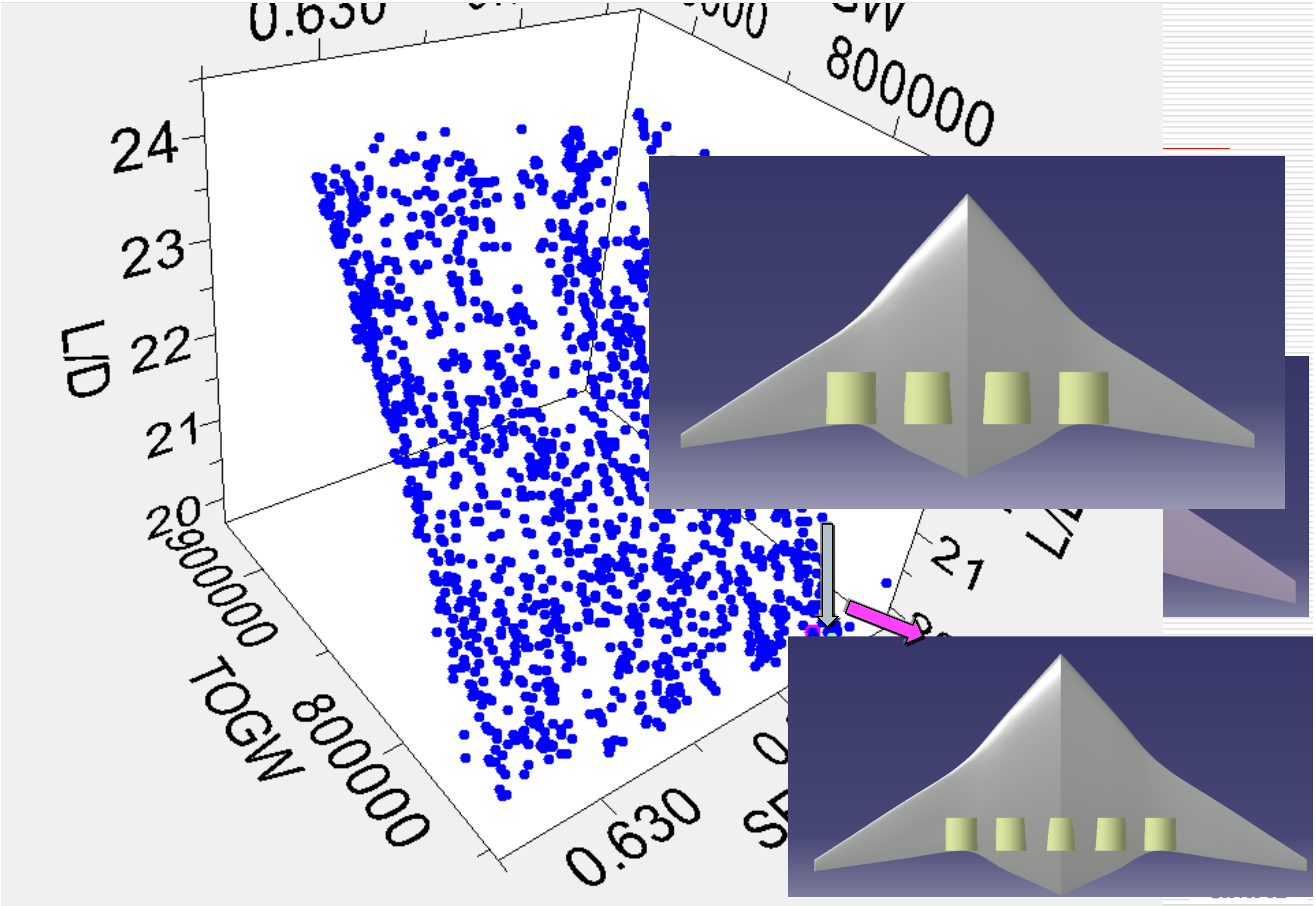
L/D
24
23
22
21
20
TOGW
900000
800000
0.630
800000
21

Engines numbers

Comparison of Aerodynamic shape with different number of engines

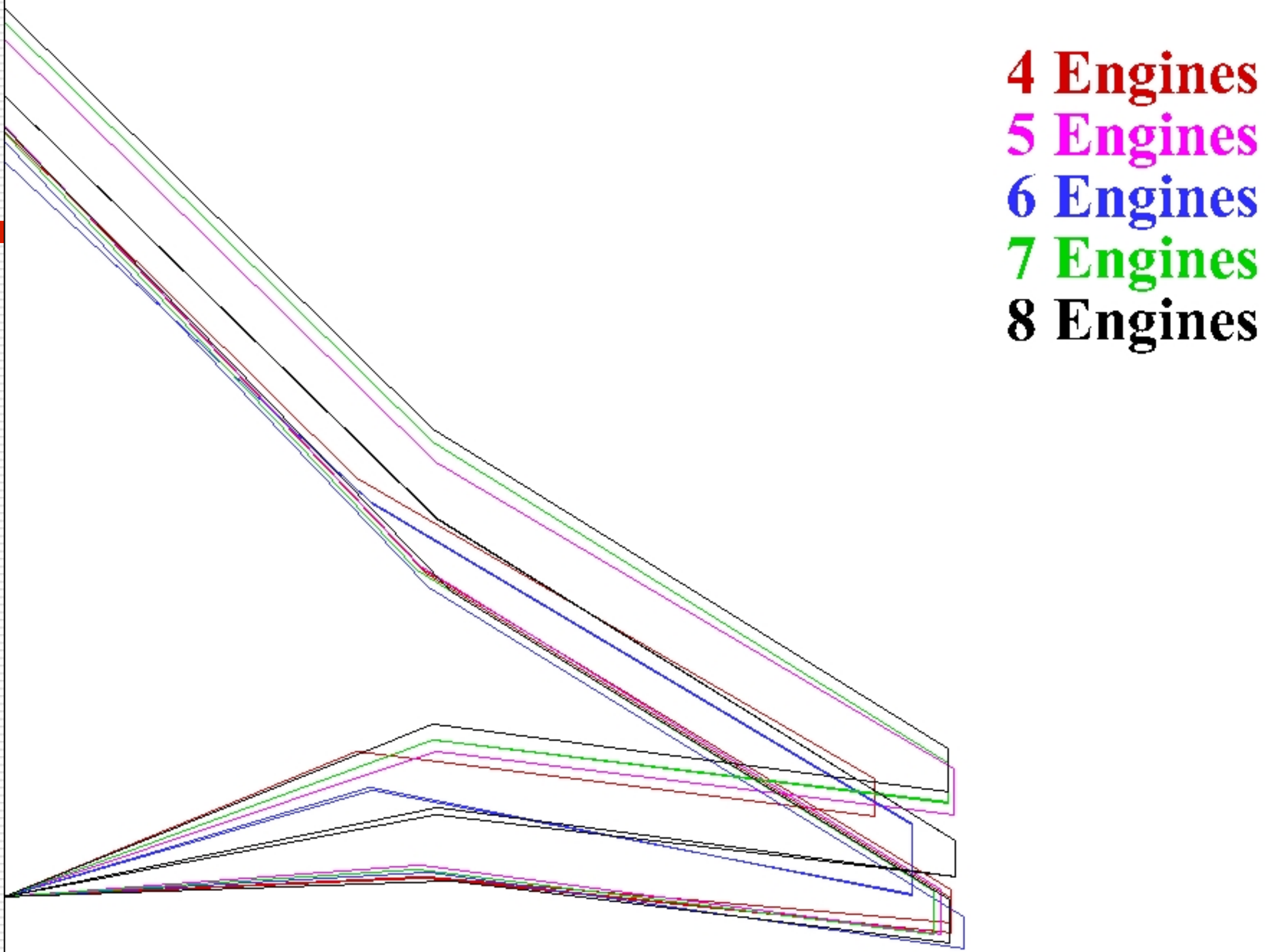

number of design variables: 15
population size: 200
total generations: 200
total CPU time: 3 hours on Intel I7 7700 CPU with 4.2GHz

Conclusion

Preliminary conclusions

Preliminary results show that the distributed propulsion BLI engine effectively:
- **shortens take off distance,**
- **improves lift coefficient and lift drag ratio, and**
- **increases maximum flight speed.**

Considering propulsion, aerodynamic and weight, the problem of multidisciplinary design optimization for distributed propulsion BWB aircraft has been solved for preliminary design .

In the optimization, the minimum take-off weight, the minimum fuel consumption rate and the maximum lift drag ratio are taken into account with 3 objective functions, combined with the constraints of flight control and voyage.

The preliminary optimization results show that the distributed propulsion layout has the advantages of improving the propulsion efficiency, improving the flight safety, reducing the induced resistance and reducing the load of the wing.

Application 3: Minimizing the Constrained Weight of Frames with Nash Genetic Algorithms: a mutation rate study

David Greiner*, Jacques Periaux**, Jose M. Emperador*, Blas Galvan*, Gabriel Winter*

*Institute of Intelligent Systems and Numerical Applications in Engineering (SIANI), Universidad de Las Palmas de Gran Canaria (ULPGC), Spain

**Department of Mathematical Information Technology (MIT), University of Jyväskyla, Finland & International Center for Numerical Methods in Engineering(CIMNE/UPC), Spain

Presented at ECFD-ECCM Congress, Glasgow, UK, 2018

Nash-Evolutionary Algorithms

A set of subpopulations co-evolve simultaneously each of which deals only with a partition of the search variables; subpopulations interact to evolve towards the equilibrium

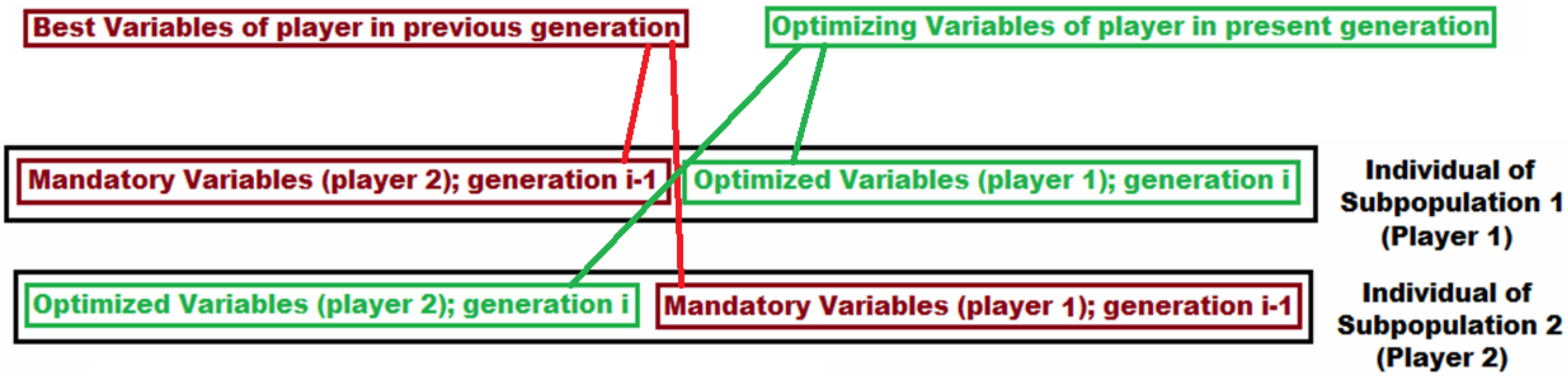

xa1 xa2 xa3 ya4 ya5 ya6	Static DD - 1
xa1 ya2 xa3 ya4 xa5 ya6	Static DD - 2
xa1 xa2 ya3 ya4 xa5 ya6	Static DD - 3
xa1 ya2 xa3 xa4 ya5 ya6	Static DD - 4

Domain Decomposition (DD):
How to distribute the assignment of variables to each subpopulation (player)

Why Evolutionary Algorithms for Structural Optimization ?

In Structural Optimization:

- Existence of local optima and disconnected domain zones.
- Both search space and variables are discrete !

Evolutionary Algorithms (EAs) are appropriate :

- are global optimizers due to their random population search.
- require no function properties (e.g: continuity, derivability, etc.)
- optimize with discrete variables

Skeletal Structures

Bar Structures are present in many engineering applications of growing interest in recent years

Structural Problem

Using the C/C++ language, the following computational implementation are developed:

- **Analyzer** : *Frame matrix calculator Program* (direct stiffness method), for Skeletal Structures.

- **Optimizer**: *Evolutionary Algorithms*(various strategies of optimization algorithms).

- Objective Function Definition (constrained weight).

Objective Function

1. The ***constrained weight***, due to minimize the acquisition cost of raw material of the metallic frame; the following constraints are applied:

   - *Stresses* of the bars (usual value for steel structures is the yield limit stress, of 2600 kgp/cm2), for each bar

$$\sigma_{co} - \sigma_{lim} \leq 0$$

   - ***Compressive slenderness limit*, (buckling effect) compression lambda lower than 200 (limit is dependendent on national codes), for each bar**

$$\lambda - \lambda_{lim} \leq 0$$

   - ***Displacements of joints or middle points* of bars (at each degree of freedom) in certain points, nodes of the beams**

$$u_{co} - u_{lim} \leq 0$$

Objective Function

The *fitness function constrained weight* has the following expression :

$$Fitness = \left[\sum_{i=1}^{Nbars} A_i \cdot \rho_i \cdot l_i \right] [1 + k \cdot \sum_{j=1}^{Nviols} (viol_j - 1)]$$

where:

A_i = area of cross-section i

p_i = density of bar i

l_i = length of bar i

k = constant that regulates the coefficient between constraint and weight.

$viol_j$ = for each of the violated constraints, is the coefficient between the violated value (stress, displacement or slenderness) and its reference limit.

Nviols = Number of constraint violations

Test Case definition (1)

Computational domain, boundary conditions, loadings and design variable set groupings:

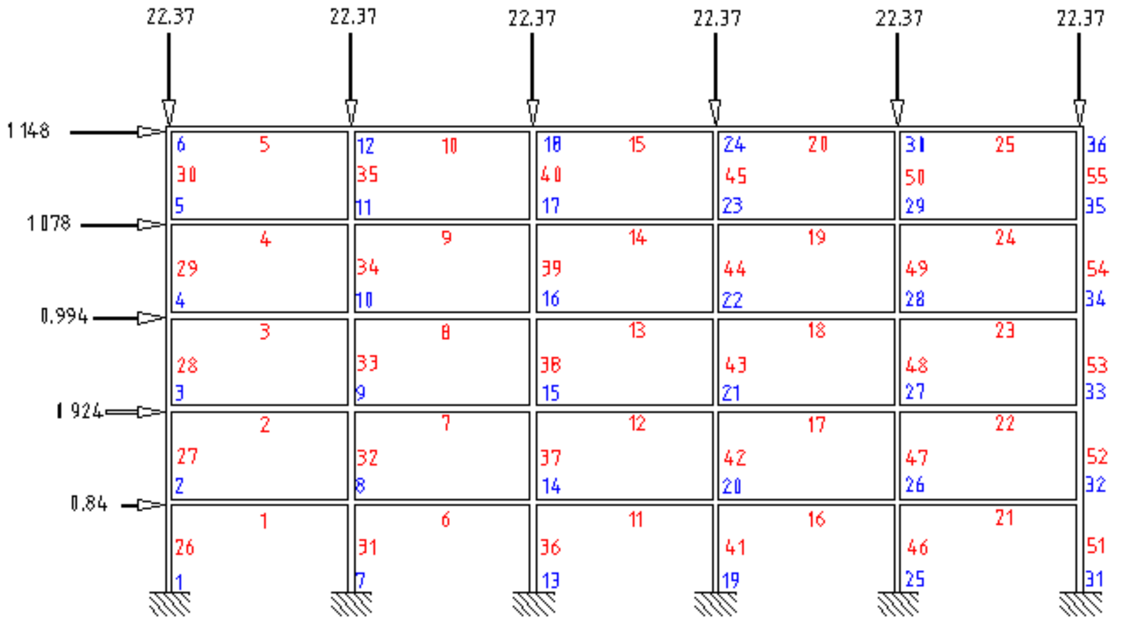

Fixed Supports

Based on (*D. Greiner, Emperador, Winter, CMAME, 2004*)

Figure includes elements and nodes numbering, and punctual loads in tons.

Every beam supports a uniform load of 39,945 N/m.

Maximum vertical displacement in each beam is l/300 = 1.86 cm.

Test Case definition (2)

- IPE cross section types for beams (set between IPE-080 and IPE-500)
- HEB for columns (set between HEB100 and HEB-450)
- Admissible stresses of 2.2 and 2.0 T/cm^2 for beams and columns, respectively.
- Density and elasticity modulus E (steel) : 7.85 T/m^3 and 2100 T/cm^2.
- Based on a continuous variable reference test problem of S. Hernández.
- The span is 5.6 m and the height of columns is 2.80 m.

55 members

Search Space: $16^{55} = 2^{4x55} = 2^{220} = 1{,}7 \cdot 10^{66}$

Fitness Function Nash EAs: MCW

Minimum Constrained Weight (MCW):

- Fitness Function in Panmictic EAs:

$$MCW = \left[\sum_{i=1}^{Nbars} A_i \cdot l_i \cdot \rho_i\right]\left[1 + k \cdot \sum_{i=1}^{Nviols} (viol_j - 1)\right]$$

- Fitness Function considering the Nash-EAs with 2 Domain Decomposition (e.g: 2 players in charge of bars):

Player 1: Nbar = 1, …, NP1
Player 2: Nbar = NP1+1, … Nbars

$$MCW = \left[\sum_{i=1}^{NP1} A_i \cdot l_i \cdot \rho_i + \sum_{i=NP1+1}^{Nbars} A_i \cdot l_i \cdot \rho_i\right]\left[1 + k \cdot \left[\sum_{j=1}^{Nviols(1,\ldots,NP1)} (viol_j - 1) + \sum_{k=1}^{Nviols(NP1+1,\ldots,Nbars)} (viol_k - 1)\right]\right]$$

Test Case: 3 domain decomposition

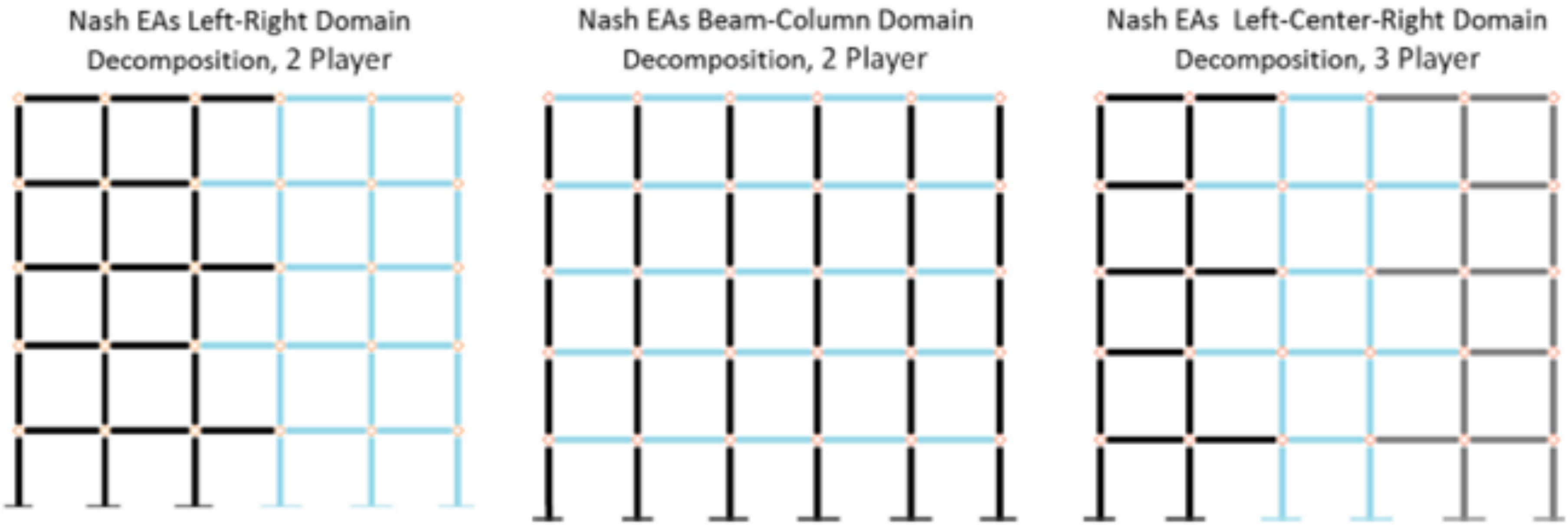

Four Algorithms Compared:

Panmicitic GA
Nash GAs Left-Right DD
Nash GAs Beam-Column DD
Nash GAs Left-Center-Right DD

Parameters:

30 independent executions
Population Size: 100
Codification: Binary Reflected Gray Code
Mutation Rates: 0.4% & 0.8%
Stopping Criterion: up to 600.000 fitness evaluations

Test Case Results: Mutation Rate Comparison MCW

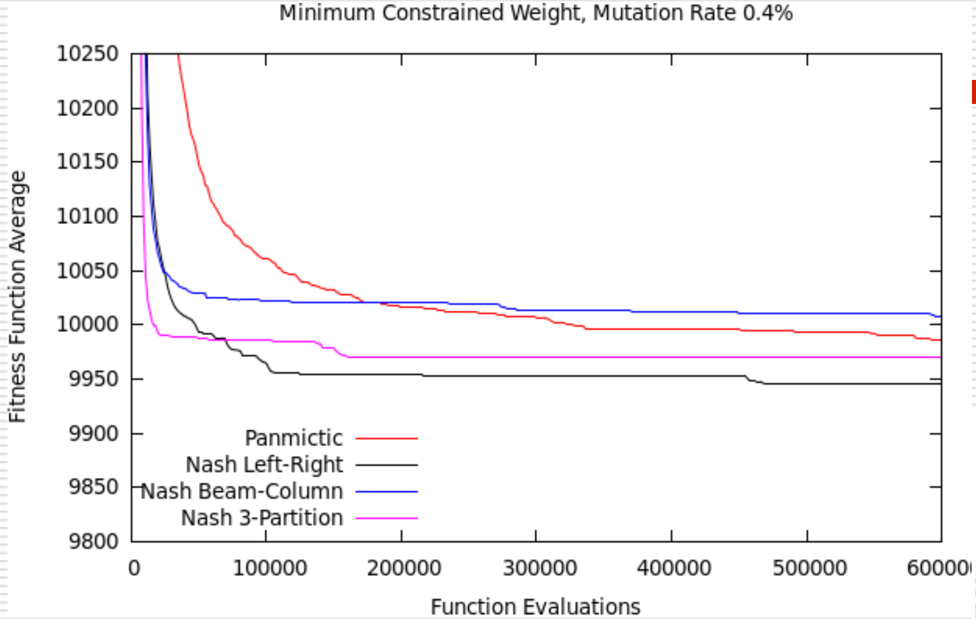

Among Nash GAs Domain Decomposition DD type has an influence in the final results

Nash strategies show a more robust behaviour with respect to mutation rate changes

Table : Generational Population Size 100. Results out of 30 independent executions; Values after 600,000 function evaluations.

Mutation Rate	Algorithm Type	Average	Median	Best	Standard Deviation
	Panmictic	9986.2	9970.4	**9852.32**	**89.1**
0.4%	Nash Left-Right	**9944.9**	**9894.1**	9852.32	95.4
	Nash Beam-Column	10007.5	10039.3	**9852.32**	116.7
	Nash 3 player	9969.6	9975.6	**9852.32**	90.9
	Panmictic	10191.9	10177.1	9949.7	142.9
0.8%	Nash Left-Right	**9918.4**	**9867.9**	9852.32	**87.3**
	Nash Beam-Column	9962.3	9959.7	**9852.32**	99.8
	Nash 3 player	9932.5	9904.8	**9852.32**	91.7

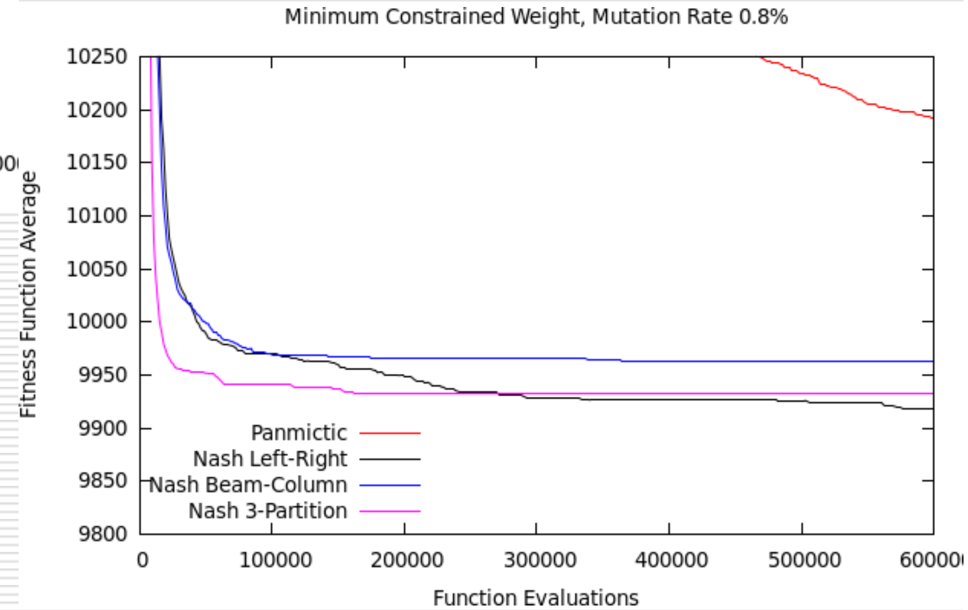

Test Case Results: Mutation Rate Comparison MCW

Among Nash GAs: Domain Decomposition DD type has influence in the final results:

Left-Right DD better than Left-Center-Right DD better than Beam-Column DD.

Nash strategies show a more robust behaviour against mutation rate changes:

In the 0.8% mutation rate, Panmictic approach worsens its behaviour, while Nash strategies are capable to maintain similar results as in the 0.4% mutation rate, even improving them in terms of average and median final values in all Nash DDs when increasing the mutation rate to 0.8%.

Benefits from increasing Population Diversity: increasing the exploration capabilities of Nash strategies is beneficial for the exploration-exploitation equilibrium, as Nash GAs inherently are increasing exploitation versus Panmictic GAs.

CIMNE

Test Case Results: The whole Set of Experiments MCW

Table: Average ranking of the algorithms (comparison based on fitness values at stopping criterion), the higher the better; Friedman Test. (p-value = $6.19 \cdot 10^{-6}$).

Algorithm	Ranking
Panmictic GA	1.87
Nash-GAs Left-Right	3.08
Nash-GAs Beam-Column	2.43
Nash-GAs 3 player	2.61

Table: Adjusted p-values, Bergmann-Hommel's posthoc procedure (comparison based on fitness values at stopping criterion).

i	Hypothesis	p-value
1	*Panmictic vs. Nash-EAs Left-Right*	*$1.77 \cdot 10^{-6}$*
2	*Panmictic vs. Nash-EAs 3 player*	*$5.59 \cdot 10^{-3}$*
3	*Nash-EAs Left-Right vs. Nash-EAs Beam-Column*	*0.017*
4	*Nash-EAs Beam-Column vs. Panmictic*	*0.036*
5	*Nash-EAs Left-Right vs. Nash-EAs 3 player*	*0.044*
6	Nash-EAs Beam-Column vs. Nash-EAs 3 player	0.458

Conclusions (this study, Minimum Constrained Weight problem):

Panmictic GAs are worse than any other Nash-GAs

Among different Nash GAs , Left-Right DD is better than other DDs

Future: What goes next ?

- Extending the analysis of game strategies based EAs to multi-objective optimization in structural engineering problems; e.g. as in handled problems:

/1/D. Greiner, G. Winter, JM. Emperador (2004) "Single and multiobjective frame optimization by evolutionary algorithms and the auto-adaptive rebirth operator", *Computer Methods in Applied Mechanics and Engineering* 193 (33), 3711-3743.

/2/D. Greiner, P. Hajela (2012) "Truss topology optimization for mass and reliability considerations —co-evolutionary multiobjective formulations", *Structural and Multidisciplinary Optimization* 45 (4), 589-613.

/3/D Greiner et al. (2013) "Engineering Knowledge-Based Variance-Reduction Simulation and G-Dominance for Structural Frame Robust Optimization", *Advances in Mechanical Engineering*, Article ID 680359, 1-13.

- Considering hybridization of multi-games like, e.g.: Stackelberg game (leader) and Nash players (several followers) in Structural Engineering

Thanks to SIANI and the XVIII Spanish-French School organizers !

Thanks for your attention ! ! !